AGAMOUS-LIKE67 Cooperates with the Histone Mark Reader EBS to Modulate Seed Germination under High Temperature[1]

Ping Li,[a,2] Qili Zhang,[a,2] Danni He,[a,2] Yun Zhou,[b] Huanhuan Ni,[a] Dagang Tian,[c] Guanxiao Chang,[b] Yanjun Jing,[d] Rongcheng Lin,[d] Jinling Huang,[b,e] and Xiangyang Hu[a,3,4]

[a]Shanghai Key Laboratory of Bio-Energy Crops, School of Life Sciences, Shanghai University, 200444 Shanghai, China

[b]State Key Laboratory of Crop Stress Adaptation and Improvement, School of Life Sciences, Henan University, Kaifeng 475004, China

[c]Biotechnology Research Institute, Fujian Key Laboratory of Genetic Engineering for Agriculture, Fujian Academy of Agricultural Sciences, Fuzhou 350003, China

[d]Key Laboratory of Photobiology, Institute of Botany, Chinese Academy of Sciences, Beijing 100093, China

[e]Department of Biology, East Carolina University, Greenville, North Carolina 27858

ORCID IDs: 0000-0001-6179-5407 (Y.Z.); 0000-0001-9905-1331 (D.T.); 0000-0002-4772-7923 (Y.J.); 0000-0001-8346-3390 (R.L.); 0000-0003-4893-4171 (J.H.); 0000-0002-8009-4419 (X.H.)

Seed germination is a vital developmental process that is tightly controlled by environmental signals, ensuring germination under favorable conditions. High temperature (HT) suppresses seed germination. This process, known as thermoinhibition, is achieved by activating abscisic acid and inhibiting gibberellic acid biosynthesis. The zinc-finger protein SOMNUS (SOM) participates in thermoinhibition of seed germination by altering gibberellic acid/abscisic acid metabolism, but the underlying regulatory mechanism is poorly understood. In this study, we report that SOM binds to its own promoter and activates its own expression in Arabidopsis (*Arabidopsis thaliana*) and identify the MADS-box transcription factor AGAMOUS-LIKE67 (AGL67) as a critical player in SOM function, based on its ability to recognize CArG-boxes within the *SOM* promoter and mediate the transactivation of *SOM* under HTs. In addition, AGL67 recruits the histone mark reader EARLY BOLTING IN SHORT DAY (EBS), which recognizes H3K4me3 at *SOM* chromatin. In response to HTs, AGL67 and EBS are highly enriched around the *SOM* promoter. The AGL67-EBS complex is also necessary for histone H4K5 acetylation, which activates *SOM* expression, ultimately inhibiting seed germination. Taken together, our results reveal an essential mechanism in which AGL67 cooperates with the histone mark reader EBS, which bridges the process of H3K4me3 recognition with H4K5 acetylation, thereby epigenetically activating *SOM* expression to suppress seed germination under HT stress.

Seed germination is a vital process in the plant life cycle and a key factor in reproductive success. Whether a seed germinates or remains dormant is strictly determined by endogenous phytohormones and environmental signals (Mazer, 1999; Donohue et al., 2005; Finch-Savage and Leubner-Metzger, 2006; Holdsworth et al., 2008; Graeber et al., 2012). Abscisic acid (ABA) and gibberellic acid (GA) are two critical phytohormones that determine the shift between dormancy and seed germination: ABA imposes seed dormancy, whereas GA induces seed germination (Kucera et al., 2005; Finkelstein et al., 2008; Shu et al., 2016). Arabidopsis (*Arabidopsis thaliana*) mutants blocked at various steps of ABA biosynthesis, such as *aba deficient1* (*aba1*) and *aba2*, *nine-cis-epoxycarotenoid dioxygenase6* (*nced6*) and *nced9*, and *abscisic aldehyde oxidase3*, have higher germination rates than wild-type seeds. Conversely, overexpression of the corresponding wild-type genes prevents seed germination (Koornneef et al., 1982; Karssen et al., 1983; Seo et al., 2004; Lefebvre et al., 2006). Seeds of mutants with defects in the ABA catabolism pathway, such as *cyp707a2*, which exhibits a loss of function in cytochrome P450 707A2, have increased seed dormancy due to elevated endogenous

[1]This work was supported by Start-up Funding from Shanghai University, Open Project Funding of the State Key Laboratory of Crop Stress Adaptation and Improvement, and the National Natural Science Foundation of China (grant no. 31970289 to X.H.) and by the Chinese Academy of Science Light of West China and National Science Foundation of China (grant no. 31970248 to J.H.).

[2]These authors contributed equally to the article.

[3]Author for contact: huxiangyang@shu.edu.cn.

[4]Senior author.

The author responsible for distribution of materials integral to the findings presented in this article in accordance with the policy described in the Instructions for Authors (www.plantphysiol.org) is: Xiangyang Hu (huxiangyang@shu.edu.cn).

X.H., J.H., and Y.Z. designed the research; P.L., Q.Z., D.H., H.N., G.C., D.T., and Y.J. performed the experiments; Y.J. and R.L. contributed the genetic tool; X.H., Y.Z., and R.L. analyzed the data; X.H. and J.H. wrote the article.

www.plantphysiol.org/cgi/doi/10.1104/pp.20.00056

ABA levels (Matakiadis et al., 2009). Similarly, seeds from mutant lines that are impaired in GA biosynthesis (e.g. the *ga requiring* [*ga*] mutants *ga1–ga5*) do not germinate well in the absence of exogenous GA (Koornneef and van der Veen, 1980; Talon et al., 1990; Sun and Kamiya, 1994; Xu et al., 1995), whereas mutants with defects in the *GA2 OXIDASE* (*GA2OX*) gene, which lack GA catabolism, show high endogenous seed GA content and reduced seed dormancy (Ogawa et al., 2003; Yamaguchi, 2008).

In addition to the ABA/GA biosynthetic pathways, the components associated with the transduction of the ABA/GA signal, such as the transcription factors ABA INSENSITIVE3 (ABI3), ABI4, and ABI5 or the DELLA-type transcriptional repressors (mainly GA INSENSITIVE [GAI], REPRESSOR OF *ga1-3* [RGA], and RGA-LIKE2 [RGL2]), also affect seed germination or dormancy (Lee et al., 2002; Penfield et al., 2006; Park et al., 2011; Dai et al., 2013; Lim et al., 2013). Furthermore, these components reciprocally affect seed germination by interfering with ABA/GA biosynthesis; for example, RGL2 binds to the *ABI5* promoter to induce *ABI5* expression, and thus ABA biosynthesis, which in turn prevents seed germination (Piskurewicz et al., 2008; Hu et al., 2019). The balance between GA and ABA levels therefore plays a crucial role in determining whether seed dormancy is maintained or seed germination is initiated.

Light and temperature are the two main environmental cues controlling seed germination and dormancy (Quail, 2002; Rajjou et al., 2012). In Arabidopsis, members of the phytochrome (phy) photoreceptor family perceive and respond to light irradiation in the red/far-red portion of the light spectrum (between 660 and 730 nm). Red light converts phy molecules into their photoactivated Pfr form and induces seed germination. By contrast, far-red light exposure converts phys back to their inactive Pr form, which suppresses seed germination (Quail, 2002; Mathews, 2006). Active phytochrome B (PhyB) interacts with the downstream basic helix-loop-helix transcription factor PHYTOCHROME-INTERACTING FACTOR1 (PIF1) to promote PIF1 degradation, modulate the expression of genes associated with ABA/GA metabolism, and initiate seed germination (Gu et al., 2017; Majee et al., 2018). The CCCH-type zinc-finger protein SOMNUS (SOM) was identified as a negative regulator of seed germination that acts downstream of PhyB. A loss-of-function *som* mutant germinates irrespective of the light conditions, even when all PhyB is inactivated by irradiation with far-red light (Kim et al., 2008; Park et al., 2011; Lim et al., 2013). Further characterization of the role of SOM in seed germination revealed that SOM activates ABA biosynthesis while repressing GA biosynthesis. Thus, *som* mutant seeds contain lower ABA but higher GA levels than wild-type seeds, conditions that promote seed germination (Chang et al., 2018).

Inhibition of seed germination by unfavorable ambient temperatures, or thermoinhibition by supraoptimal conditions, is a common limitation of many winter annual or biennial species that prevents germination under adverse environments (Toh et al., 2008; Auge et al., 2015). High temperatures (HTs) induce the expression of ABA biosynthetic genes or signaling components, such as *NCED4*, *NCED9*, and *ABI5*, and inhibit seed germination in Arabidopsis and lettuce (*Lactuca sativa*) seeds. Thermoinhibition of seed germination can, however, be alleviated by treating seeds with ABA biosynthetic inhibitors or providing them with exogenous GA (Argyris et al., 2008; Toh et al., 2008; Schwember and Bradford, 2010; Huo et al., 2013). By contrast, seed germination of *aba2* and *abi3* mutants is not disrupted by HT stress (Toh et al., 2008; Yang et al., 2019). HTs also activate *SOM* expression, which prevents seed germination by increasing ABA seed content and reducing GA biosynthesis. This step requires functional ABA and GA biosynthetic pathways, as the transcription factors ABI3, ABI5, and DELLA can target the *SOM* promoter and induce *SOM* expression during HT stress (Lopez-Molina et al., 2003; Lim et al., 2013; Yang et al., 2019). We recently demonstrated that ABI5 BINDING PROTEIN2 (AFP2) enhanced HT tolerance with respect to seed germination by interfering with the ABI5 signal (Garcia et al., 2008; Chang et al., 2018). In addition to affecting transcription, HTs disturb the activity of the epigenetic factor POWERDRESS (PWR) and modify histone H3 deacetylation levels and deposition of the histone H2A variant H2A.Z at the *SOM* locus, ultimately activating ABI3-dependent *SOM* expression and thereby blocking seed germination (Yang et al., 2019). These data suggest that SOM, as an essential negative regulator of seed germination, is strictly controlled by HTs at multiple points; however, the underlying mechanism has yet to be fully elucidated.

Apart from seed germination and dormancy, tolerance to seed desiccation is a central adaptive trait for terrestrial plants that allows plant seeds to remain viable in a dry state for several years, sometimes even centuries, and to resume germination after rehydration. Integrative genomics, bioinformatics, and metabolomics analyses highlighted the role of two specific transcriptional subnetworks in this process. The transcription factors PLATZ1 and PLATZ2 (for plant AT-rich sequence- and zinc-binding protein) and AGAMOUS-LIKE67 (AGL67) are key nodes in these networks; their respective mutants exhibited lower seed desiccation tolerance, whereas overexpression of their encoding genes enhanced the desiccation tolerance of the strong *abi3-5* mutant, demonstrating their function in seed desiccation tolerance (González-Morales et al., 2016). AGL67 also regulates seed dormancy, as the *agl67* mutant shows reduced seed dormancy. Genetic analysis indicated that *AGL67* interacts with *EARLY BOLTING IN SHORT DAY* (*EBS*), and both genes may belong to a common pathway to control seed dormancy (Narro-Diego et al., 2017). EBS possesses a bivalent bromo-adjacent homology (BAH)-plant homeodomain (PHD) and functions as a reader of histone marks that binds specifically to H3K4me2 and H3K4me3 in vitro

(Piñeiro et al., 2003; López-González et al., 2014; Yang et al., 2018). These observations suggest that EBS may control seed dormancy at the epigenetic level, but whether the AGL67-EBS module controls the thermoinhibition of seed germination through *SOM* has not been determined.

In this study, we aimed to further elucidate the molecular mechanism of SOM function during thermoinhibition of seed germination. A series of biochemical methods revealed that SOM interacted with AGL67 and EBS as a complex to epigenetically activate *SOM* expression through reading the H3K4me3 mark and H4K5 acetylation. Genetic and physiological analyses showed that the AGL67-EBS module coordinated SOM activity and downstream GA/ABA metabolism, ultimately suppressing seed germination under HT. Thus, our study extends previous knowledge of AGL67 function and provides insight into the molecular mechanism that couples a transcription factor, a reader of histone methylation, and a change in chromatin structure through histone acetylation during thermoinhibition of seed germination.

RESULTS

SOM Binds to Its Own Promoter to Facilitate Its Transcription

To investigate the transcriptional machinery upstream of *SOM*, we initially screened for putative trans-acting factors in the promoter region of *SOM* by a yeast one-hybrid (Y1H) assay. With this goal in mind, we first wished to identify a minimal SOM promoter that would fully complement the *som-2* mutant when driving the expression of *SOM*. To this end, we fused the coding region of *SOM* to a FLAG tag and placed the gene under the control of a 2.4-kb fragment upstream of its start codon as the native promoter (*SOMpro*:*SOM-FLAG*, abbreviated as *SOM-FLAG*). We detected a strong signal in individual transgenic seeds expressing *SOM-FLAG* by immunoblot analysis (Supplemental Fig. S1A). We then introduced *SOM-FLAG* into the *som-2* mutant to generate complementation lines. HT treatment of 32°C blocked seed germination in wild-type Columbia-0 (Col-0) as well as *SOM-FLAG som-2* but not *som-2* (Fig. 1, A and B), demonstrating effective complementation of *som-2* by the *SOM-FLAG* construct in the context of germination thermotolerance. These results also indicate that the 2.4-kb *SOM* promoter fragment bears sufficient cis-acting elements to drive adequate *SOM* expression and rescue *som-2*. Furthermore, HT induced SOM-FLAG protein accumulation in transgenic *SOM-FLAG* seeds during the first 24 h of HT exposure, followed by a slight drop after 36 h (Fig. 1C). These results agree with the published effects of HT on *SOM* expression (Lim et al., 2013).

To identify the trans-acting factors that control *SOM* expression, we used this 2.4-kb fragment as a bait in a Y1H assay to screen an Arabidopsis normalized cDNA library. One of the positive clones isolated during the screen was SOM itself, suggesting that SOM might bind to its own promoter and control its own expression. We independently confirmed the strong binding of SOM to this 2.4-kb promoter fragment by retransforming yeast cells. We also tested each half of the 2.4-kb *SOM* promoter for SOM binding and only saw evidence of binding between SOM and the proximal 1.2-kb fragment (P-SOM) but not the distant 1.2-kb fragment (D-SOM; Fig. 1D).

The *SOM* promoter is A/T-rich, and tandem zinc finger (TZF) proteins like SOM preferentially bind to AU-rich elements in the 3′ untranslated regions of mRNAs to trigger their degradation (Laity et al., 2001; Jang, 2016). We reasoned that SOM, also known as TZF4, might also bind these A/T-rich regions (Kim et al., 2008). Using a chromatin immunoprecipitation (ChIP)-quantitative PCR (qPCR) assay, we established that the C3 and C4 fragments within the proximal fragment of the *SOM* promoter were dramatically enriched after pull-down with an anti-FLAG antibody (Fig. 1E). Thus, these data suggest that SOM binds to its own promoter, somewhere along the proximal 1.2 kb immediately upstream of the ATG.

We also generated transgenic *SOMpro*:*GUS* reporter lines that placed the *GUS* gene under the control of the 2.4-kb *SOM* promoter. We detected a strong GUS signal in Col-0 seeds bearing the *SOMpro*:*GUS* reporter (Fig. 2A) but a much reduced GUS signal when *SOMpro*:*GUS* was introduced into the *som-2* mutant background (*SOMpro*:*GUS/som-2*). The transgenic lines that overexpressed SOM as a GFP fusion under the control of the cauliflower mosaic virus 35S promoter (*35Spro*:*SOM-GFP*, referred to as *SOM-GFP*; Supplemental Fig. S1B) was generated, and the *SOMpro*:*GUS* reporter was introduced into *SOM-GFP* lines by genetic crossing to obtain *SOMpro*:*GUS SOM-GFP* double transgenic lines. Reverse transcription (RT)-qPCR analysis revealed that *GUS* expression was lower in *SOMpro*:*GUS som-2* seeds but much higher in *SOMpro*:*GUS SOM-GFP* double transgenic seeds (Fig. 2B). Thus, these results confirm that SOM activates its own expression.

AGL67 Binds to the *SOM* Promoter and Activates *SOM* Expression

During our Y1H screen, we also established that the MADS-box transcription factor AGL67 associates with the *SOM* promoter, specifically to the proximal 1.2-kb *SOM* promoter fragment (*P-SOM*; Supplemental Data Set S1; Supplemental Fig. S2, A and B). To infer the function of AGL67, we assessed the expression pattern of *AGL67* in the Arabidopsis eFP browser (http://bar.utoronto.ca/efp/cgi-bin/efpWeb.cgi). *AGL67* is only and strongly expressed in dry seeds or during late seed development (Supplemental Fig. S3). Consistent with these in silico data, the GUS staining pattern of *AGL67pro*:*GUS* transgenic lines (expressing *GUS* under the control of the *AGL67* promoter) was strong in

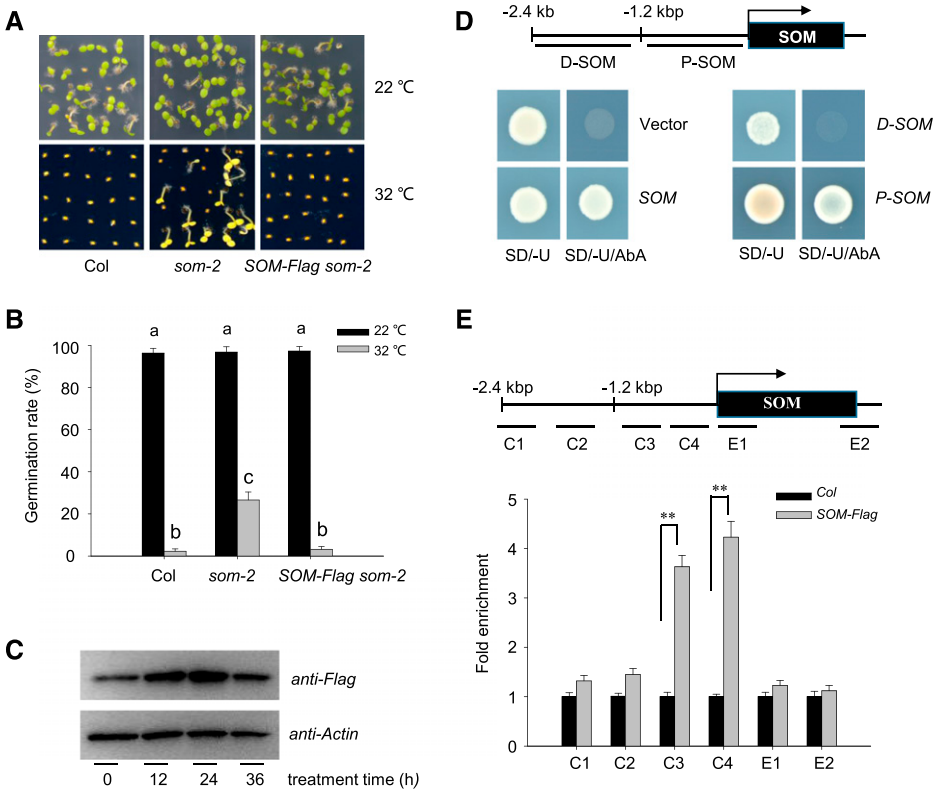

Figure 1. Identification of putative trans-regulatory factors of *SOM* expression. A and B, Seed germination phenotype of Col-0, *som-2*, and its complementation line (*SOM-FLAG som-2*) under normal conditions (22°C) or HT stress (32°C). Hydrated seeds were germinated on one-half-strength Murashige and Skoog medium with 1% (w/v) agar at 22°C or 32°C. Photographs were taken after 10 d (A). The experiment was repeated three times with similar results. Seed germination rates were calculated after 5 d (B). Values are means ± SD of three biological replicates; bars labeled with different letters are significantly different at $P < 0.05$ (Tukey's test). C, HT increases SOM protein abundance in hydrated seeds. Seeds from *SOM-FLAG som-2* were treated at 32°C for 0 to 36 h, and total protein extracts from hydrated seeds were analyzed by immunoblot with an anti-FLAG antibody. Actin was used as the loading control. The experiments were repeated three times, with similar results. D, SOM binds to its own promoter. The 2.4-kb *SOM* promoter fragment was cloned into the pABAi vector (pABAi-SOM, indicated as SOM) or the 2.4-kb fragment was evenly divided into a 5′ or 3′ fragment of 1.2 kb length each (pABAi-D-SOM and pABAi-P-SOM, indicated as D-SOM and P-SOM, respectively). The full-length SOM was fused to the pGBKT7 vector. Yeast cells were cotransformed with the combinations of various pABAi and pGBKT7 and grown on synthetic dropout (SD) medium lacking Ura (SD/-U) or lacking Ura but additionally aureobasidin A (SD/-U/AbA). The binding ability of SOM with the 2.4-kb promoter or the 1.2-kb proximal fragment is indicated by growth on the SD/-U/AbA plate. A diagram of the 2.4-kb fragment or the 1.2-kb distal (*D-SOM*) or proximal (*P-SOM*) fragment of the *SOM* promoter is shown on top. E, ChIP-qPCR analysis of the binding ability of SOM to its own promoter. Hydrated *SOM-FLAG* transgenic seeds and wild-type Col-0 seeds were used for ChIP-qPCR using an anti-FLAG antibody. *ACTIN2* served as an internal control. Enrichment was normalized to the level of input DNA. Values are shown as means ± SD of triplicate experiments. Asterisks indicate significant difference by Student's *t* test (**$P < 0.01$). The top diagram indicates the genomic structure of *SOM*. Black boxes indicate exons. P1 to P4, E1, and E2 fragments show PCR regions amplified during ChIP.

siliques, germinated seeds, and mature embryos but weaker in young seedlings and mature leaves (Fig. 2C), indicating its potential role in seed germination.

To determine whether AGL67 is required for *SOM* expression, we obtained two T-DNA insertion mutants, *agl67-1* and *agl67-2*. In *agl67-1*, the T-DNA had inserted into the first intron of *AGL67*, while *agl67-2* carried the T-DNA in the third exon of *AGL67*. Both alleles abolished the accumulation of a functional *AGL67* transcript (Supplemental Fig. S4). We then crossed *agl67-1* and *agl67-2* to our *SOMpro:GUS* reporter line. GUS staining was clearly lower in *SOMpro:GUS agl67-1* or *SOMpro:GUS agl67-2* hydrated seeds compared with *SOMpro:GUS* seeds in the Col-0 background (Fig. 2D). RT-qPCR analysis showed that HT stress gradually increased the expression of *AGL67* and *SOM* (Fig. 2E; Supplemental Fig. S5A), but the HT-induced increase of *SOM* transcript levels was compromised in the *agl67-1* or *agl67-2* mutants (Fig. 2E). Collectively, these data suggest that AGL67 binding to the *SOM* promoter is necessary to activate *SOM* expression.

To identify which region of the *SOM* promoter is necessary for AGL67 binding, we divided the 1.2-kb proximal *SOM* promoter into a series of smaller fragments and tested their interaction with AGL67 by Y1H analysis. As shown in Supplemental Figure S2C, the C3

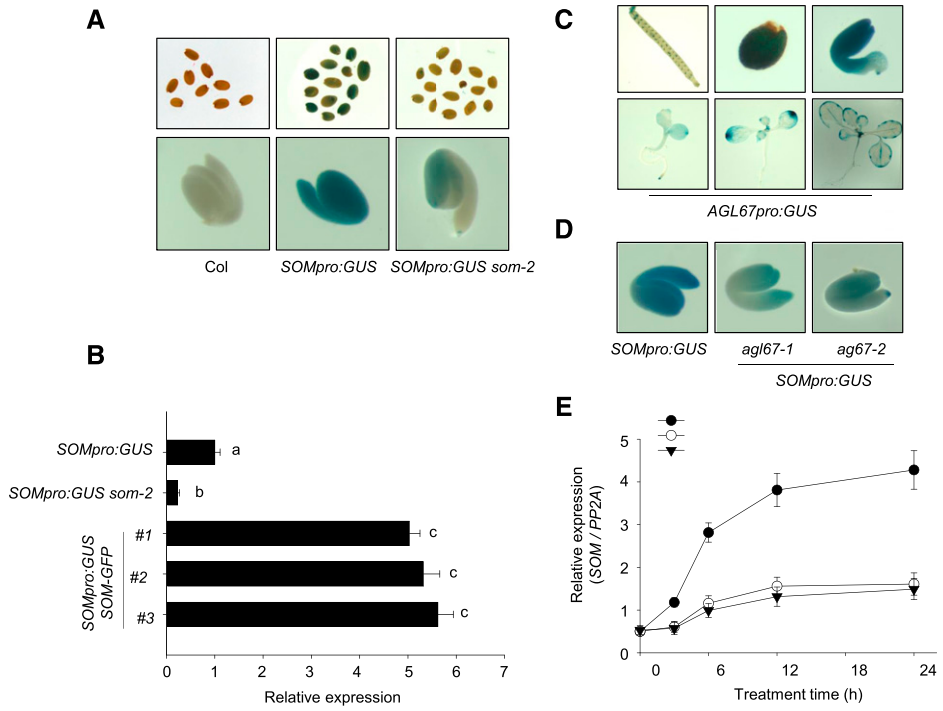

Figure 2. Expression pattern of *SOM* and *AGL67*. A, GUS staining of freshly harvested *SOMpro*::*GUS* transgenic seeds in the Col-0 and *som-2* backgrounds. Nontransgenic Col-0 was used as a control. All seeds were hydrated for 12 h before GUS staining. The top row shows intact seeds, and the bottom row shows embryos after the removal of seed coat and endosperm. B, RT-qPCR analysis of GUS transcripts in *SOMpro*:*GUS* hydrated seeds in Col-0, *som-2* mutant, and *SOM-GFP* backgrounds. All seeds were hydrated in water for 12 h. *PROTEIN PHOSPHATASE2A* (*PP2A*) was used for normalization. Values are means ± SD of three biological replicates; bars labeled with different letters are significantly different at $P < 0.05$ (Tukey's test). C, GUS staining of the *AGL67pro*:*GUS* line in wild-type seeds. D, Effects of *AGL67* genotype on *SOMpro*:*GUS* staining pattern in the seed embryo. Freshly harvested seeds of transgenic *SOMpro*:*GUS* Col-0 and *agl67-1* and *agl67-2* mutants were hydrated for 12 h before GUS staining. The seed coat and endosperm were removed before capturing photographs of embryos. E, RT-qPCR analysis of *SOM* transcript levels in hydrated seeds of *SOMpro*:*GUS* in wild-type Col-0, *agl67-1*, and *agl67-2* backgrounds. All seeds were hydrated at 32°C for 0 to 24 h. *PP2A* was used for normalization. Values are shown as means ± SD from three biological replicates.

fragment was the smallest fragment to interact with AGL67 in yeast cells. In plants, MADS-box transcription factors recognize the cis-element CArG (C-[A/T] rich-G) within the promoter of target genes to regulate their expression (Castelán-Muñoz et al., 2019). Bioinformatic analysis of the 1.2-kb proximal *SOM* promoter fragment revealed 22 candidate CArG-box motifs (labeled as cis-a to cis-v in Supplemental Fig. S2C). To establish which CArG-box(es) contribute to AGL67 binding in planta, we performed a ChIP assay using transgenic seeds that overexpress *AGL67-FLAG* from the 35S promoter (*35Spro*:*AGL67-FLAG*, termed *AGL67-FLAG*; Supplemental Fig. S1C) and assessed several regions spanning different CArG motifs. The P3 region, which is included within the C3 fragment identified earlier through Y1H screening, was highly enriched in the pull-down with an anti-FLAG antibody (Fig. 3A). Thus, the P3 region is important for the association of AGL67 with the *SOM* promoter.

There are two canonical CArG cis-elements (termed cis-*j* and cis-*k*) within the P3 region. An electrophoretic mobility shift assay (EMSA) revealed that AGL67 formed a complex with labeled probes containing the cis-*j* or cis-*k* element, as evidenced by a shift in mobility (Fig. 3B). The interaction was specific to the CArG motif, as (1) the shift in mobility was gradually competed by the addition of cold probes and (2) mutated labeled probes without a CArG motif did not associate with AGL67 (Fig. 3B). AGL67 therefore binds to the *SOM* promoter by recognizing the cis-*j* and cis-*k* CArG motifs.

To assess the effect of AGL67 on *SOM* expression in vivo, we performed transient expression assays in Arabidopsis protoplasts. The effector consisted of AGL67 or SOM under the control of the *35S* promoter, while the reporters contained the firefly (*Photinus pyralis*) luciferase gene under the control of a 2.4-kb *SOM* promoter (*SOMpro*:*LUC*) or promoter variants lacking various CArG motifs (Fig. 3, C and D). AGL67 activated the expression of the *SOMpro*:*LUC* reporter in Arabidopsis protoplasts, and SOM cooperated with AGL67 to further enhance the expression of the *SOMpro*:*LUC* reporter. AGL67 also activated the expression of *SOMproP*:*LUC* (driving *LUC* under the control of the proximal *SOM* promoter) or *SOMproPΔP4*:*LUC* (driving *LUC* under the control of the proximal *SOM*

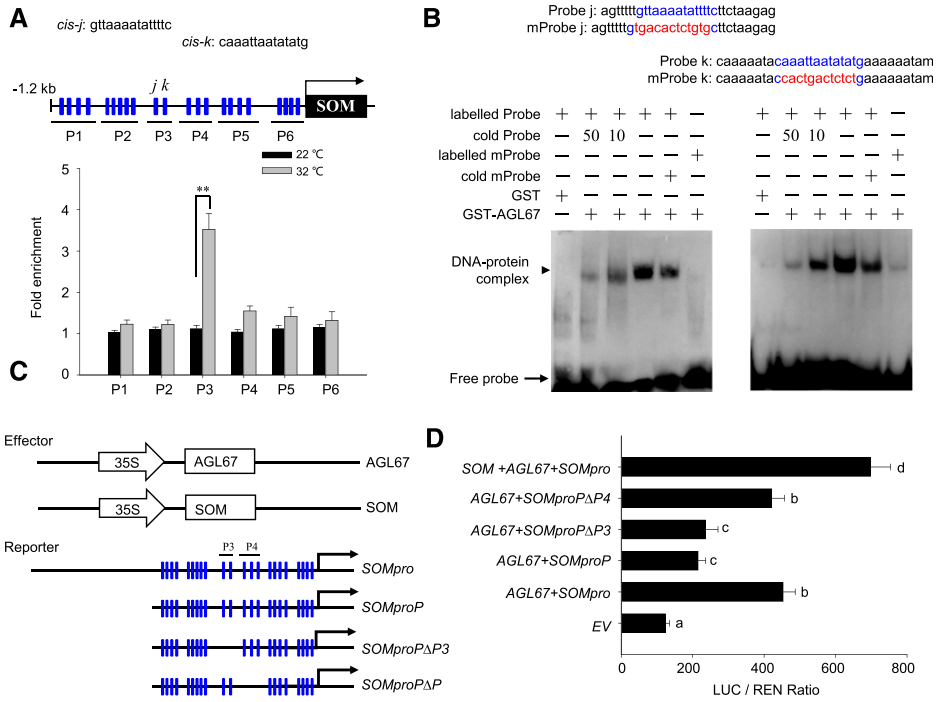

Figure 3. AGL67 binds to the *SOM* promoter to activate *SOM* expression. A, ChIP-qPCR assay of the association of AGL67 with the *SOM* promoter in vivo. Hydrated Col-0 or AGL67-FLAG seeds were used. Top, Diagram of the *SOM* promoter showing the positions of CArG-boxes (blue rectangles) and six regions (P1–P6) for ChIP-qPCR amplification, as indicated by black lines under the CArG-boxes. The sequences of the *cis-j* and *cis-k* elements within the P3 fragment are shown above. Bottom, Fold enrichment of six amplified fragments as quantified by qPCR. Anti-FLAG antibody was used for ChIP. *ACTIN2* served as an internal control, and enrichment values were normalized to the level of input DNA. Values are shown as means ± SD of triplicate experiments. Asterisks indicate significant difference by Student's *t* test (**$P < 0.01$). B, EMSA verification of the direct binding of AGL67-GST protein to the probe containing the *cis-j/k* elements in vitro. Labeled probe is a 30-bp biotin-labeled probe containing the cis-*j* and cis-*k* elements and CArG motif (highlighted in blue). Probe sequences are shown on top: cold probe, unlabeled wild-type probe (the 10- or 50-fold cold probe was used to compete the specific binding of the labeled probe to the cis-*j* and cis-*k* elements); labeled mProbe, 30-bp biotin-labeled mutated probe containing a mutated CArG motif (highlighted in red); cold mProbe, unlabeled mutated probe. The black arrows point to DNA/protein complexes and free probe, as indicated. C, Schematic diagram of the effector and reporter constructs used in the transient transfection activity assay. The positions of the CArG-boxes (blue rectangles) are indicated in the reporters containing different truncated *SOM* promoters. D, AGL67 activates the *SOM* promoter. Full-length or truncated versions of the *SOMpro:LUC* reporter were coexpressed with AGL67 or SOM effectors for 24 h; the firefly luciferase and renilla luciferase (LUC/REN) ratio represents *SOMpro:LUC* activity relative to the internal control (*35Spro:REN*). Data are means ± SD of three biological replicates. Bars with different letters are significantly different at $P < 0.05$ (Tukey's test).

promoter with a deletion of the P4 region) but not when the P3 region was deleted from the proximal SOM promoter (*SOMproPΔP3:LUC*). These observations further confirmed that AGL67 specifically recognizes the cis-*j* and cis-*k* elements in the P3 region to activate *SOM* expression in planta.

SOM Interacts with AGL67 in Vitro and in Vivo

Considering that SOM and AGL67 bind to the same region of the *SOM* promoter, we speculated that SOM might form a complex with AGL67 to coordinate *SOM* expression. To test this hypothesis, we first confirmed the interaction between AGL67 and SOM in a yeast two-hybrid (Y2H) assay (Fig. 4A). Pull-down analysis also showed that His-SOM (SOM with an N-terminal His tag) was coimmunoprecipitated by GST-AGL67 (AGL67 with an N-terminal GST tag) but not by GST alone in vitro (Fig. 4B).

We then performed a bimolecular fluorescence complementation (BiFC) analysis to test the interaction of SOM and AGL67 in planta. As shown in Figure 4D, strong YFP fluorescence was observed in the nuclei of epidermal cells transiently coexpressing *AGL67-nYFP* and *SOM-cYFP* in *Nicotiana benthamiana* leaves. We did not detect YFP fluorescence in the control experiments, in which *AGL67-nYFP* was transiently coexpressed with empty *cYFP* or *SOM-cYFP* was transiently coexpressed with empty *nYFP*. As confirmation, we performed a coimmunoprecipitation (Co-IP) assay using a total protein extract from *AGL67-GFP SOM-FLAG* or *GFP SOM-FLAG* hydrated seeds with an anti-GFP antibody. In agreement with the BiFC results, SOM-FLAG was pulled down with AGL67-GFP but not with GFP alone (Fig. 4C). Taken together, these results

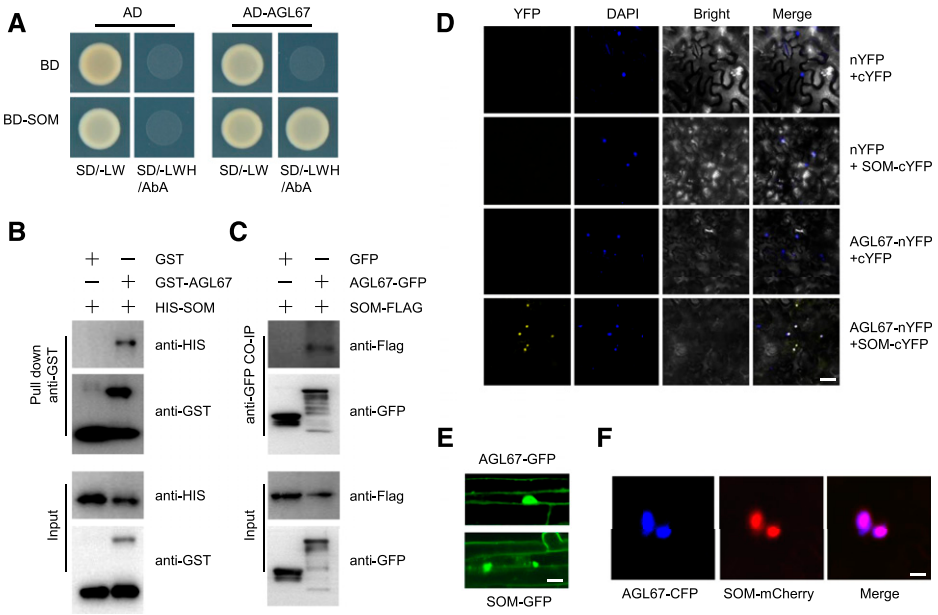

Figure 4. AGL67 physically interacts with SOM in vitro and in vivo. A, Y2H analysis of the interaction between AGL67 and SOM. Yeast cells cotransformed with the indicated construct combinations were grown on SD medium lacking Trp/Leu (-LW) or Trp/Leu/His (-LWH) with 100 ng mL^{-1} aureobasidin A (AbA). AD, DNA-activation domain of GAL4; BD, DNA-binding domain of GAL4. B, Pull-down assay showing direct interaction between His-SOM and GST-AGL67 fusion proteins in vitro. His-SOM proteins were incubated with immobilized GST or GST-AGL67 proteins. Immunoprecipitated fractions were detected by anti-His or anti-GST antibody, as indicated. C, CoIP showing the interaction of AGL67 and SOM in Arabidopsis. Plant protein extracts from hydrated seeds from *AGL67-GFP SOM-FLAG* were immunoprecipitated by GFP-Trap beads. The coimmunoprecipitated proteins were detected by anti-FLAG or anti-GFP antibody. Immunoblots show the presence of proteins in total protein extracts of plants (input) and fractions after immunoprecipitation by anti-FLAG or anti-GFP. Total protein from *GFP SOM-FLAG* was used as a negative control. D, BiFC assay showing that AGL67-cYFP interacts with SOM-nYFP in the nucleus of *N. benthamiana* epidermal leaf cells. AGL67 was fused to the N-terminal fragment of YFP (nYFP) to form AGL67-nYFP. SOM was fused with the C-terminal fragment of YFP (cYFP) to generate SOM-cYFP. YFP fluorescence was detected in *N. benthamiana* leaves coinfiltrated with the indicated constructs. Nuclei were stained with 4,6-diamidino-2-phenylindole (DAPI). Bar = 50 μm. E, Subcellular localization of AGL67 and SOM in the hypocotyl of *AGL67-GFP* (top) and *SOM-GFP* (bottom) seedlings. Bar = 10 μm. F, AGL67-CFP and SOM-mCherry colocalize in the nucleus of *N. benthamiana* epidermal leaf cells. Bar = 5 μm.

demonstrate that AGL67 interacts with SOM in vitro and in vivo.

Using the transgenic *AGL67-GFP* lines, we examined the localization of AGL67. We observed strong GFP fluorescence in the nucleus as well as a weaker signal at the plasma membrane (Fig. 4E). Similarly, we observed strong GFP fluorescence in nuclei of *SOM-GFP* transgenic lines (Fig. 4E). AGL67 and SOM colocalized to the nucleus of *N. benthamiana* leaves transiently coexpressing *AGL67-CFP* and *SOM-mCherry* under the control of the *35S* promoter (Fig. 4F). These results all suggest that AGL67 and SOM physically interact in the nucleus.

AGL67 Negatively Controls Seed Germination through SOM under HT Stress

Having established that AGL67 interacts with SOM, we reasoned that AGL67 might control seed germination by modulating *SOM* expression. To test this hypothesis, we measured seed germination rates in Col-0, *agl67* mutants, and the *AGL67-FLAG* line. Gradually increasing ambient temperature suppressed the germination of Col-0 seeds, whereas *agl67* mutant seeds exhibited a higher germination rate at the same temperatures. Conversely, the germination rate of *AGL67-FLAG* was lower than that of Col-0 seeds under the same HT conditions (Fig. 5A). Thus, we propose that AGL67 negatively regulates seed germination thermotolerance.

To explore the genetic relationship between AGL67 and SOM, we next crossed the *AGL67-FLAG* line with the *som-2* mutant to generate *AGL67-FLAG som*; we also crossed the *agl67-1* mutant with *SOM-GFP* to generate *SOM-GFP agl67* (Supplemental Fig. S5, B and C). Under HT stress at 32°C, the seed germination rates of *SOM-GFP* and *AGL67-FLAG* were lower than those of *som-2* or *agl67-1* (Fig. 5B). By contrast, *AGL67-FLAG som* and *som-2* seeds both showed relatively higher and similar germination rates. Although the *agl67-1* mutant germinated better than Col-0 under HT (Fig. 5A), both *SOM-GFP* and *SOM-GFP agl67* had even lower germination rates than those observed for Col-0 (Fig. 5B). As

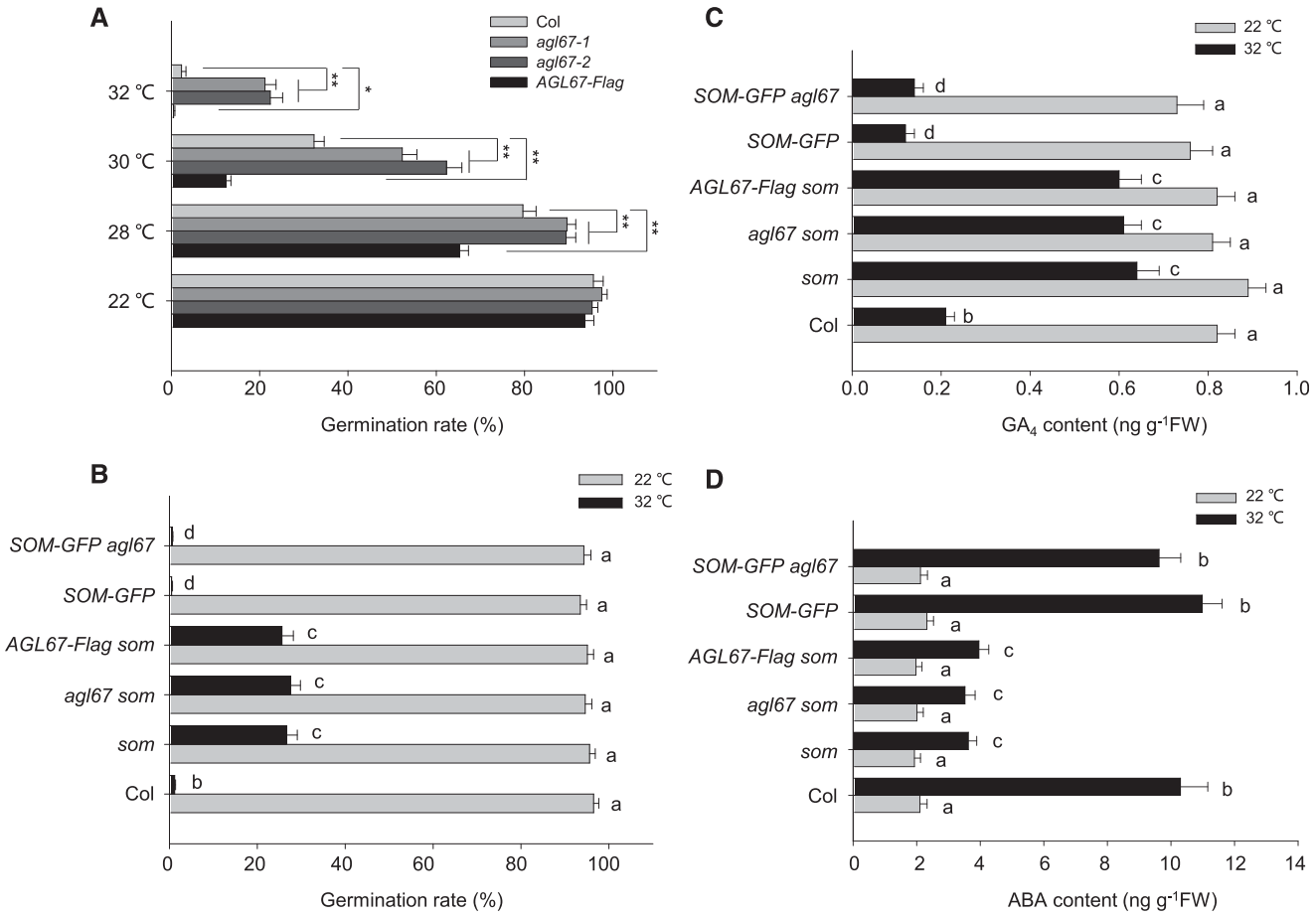

Figure 5. Regulation of seed germination thermotolerance by AGL67 and SOM. A, Seed germination rates in Col-0, *agl67* mutants, and *AGL67-FLAG* lines. Seeds were surface sterilized and plated on solid one-half-strength Murashige and Skoog medium before being released at different high temperatures as indicated. Seed germination rates were recorded after 5 d of treatment. For each biological replicate, we tested the seeds (more than 100) from the same batch, and three technical replicates were conducted for statistical analysis. Values represent means ± SD from three biological replicates. Asterisks indicate significant difference by Student's *t* test (**$P < 0.01$ and *$P < 0.05$). B, SOM is epistatic to AGL67 in the control of seed germination inhibition at high temperatures. Seeds from Col-0, *som*, *agl67 som*, *AGL67-FLAG som*, *SOM-GFP*, and *SOM-GFP agl67* were surface sterilized and plated on solid one-half-strength Murashige and Skoog medium before being released at 22°C or 32°C. Seed germination rates were recorded after 5 d of treatment. Values are means ± SD of three biological replicates; bars labeled with different letters are significantly different at $P < 0.05$ (Tukey's test). C and D, GA_4 and ABA contents in hydrated seeds. All seeds were germinated either at 22°C or 32°C, and the content of GA_4 or ABA was measured after 3 d of treatment. Values are means ± SD of three biological replicates; bars labeled with different letters are significantly different at $P < 0.05$ (Tukey's test).

loss of AGL67 (as in *agl67-1*) had no effect on the germination rate of *SOM-GFP* under HT stress, these data suggest that SOM acts downstream of AGL67. Thus, *SOM* is epistatic to *AGL67* and AGL67 targets SOM to control seed germination under HT stress.

Considering that SOM regulates seed germination by altering GA/ABA metabolism (Kim et al., 2008; Lim et al., 2013; Chang et al., 2018), we next examined whether AGL67 affects GA/ABA levels after exposure to HT stress. The seed content of the bioactive form GA_4 decreased in all genotypes (Col-0, *SOM-GFP*, and *SOM-GFP agl67*) when subjected to HT stress, but this reduction was not as pronounced in *som-2*, *agl67 som* double mutants, or *AGL67-FLAG som* (Fig. 5C). By contrast, the ABA content of Col-0, *SOM-GFP*, and *SOM-GFP agl67* seeds increased after HT stress, although the same HT stress only modestly raised the ABA content in *som-2*, *agl67 som*, and *AGL67-FLAG som* seeds (Fig. 5D). Consistent with this pattern, transcript levels of two GA biosynthesis genes (*GA3ox1* and *GA3ox2*) and one ABA catabolic gene (*CYP707A2*) were higher in *agl67*, *som-2*, and *AGL67-FLAG som* relative to Col-0 or *AGL67-FLAG* after HT stress. Conversely, transcript levels of the GA catabolic gene *GA2ox2* and ABA biosynthesis genes *ABA1*, *NCED6*, and *NCED9* were relatively lower in *agl67*, *som-2*, and *AGL67-FLAG som* than in Col-0 or *AGL67-FLAG* seeds (Supplemental Fig. S6). These data collectively support our conclusion that AGL67 does affect GA/ABA metabolism, possibly through SOM.

The Histone Reader EBS Negatively Controls Seed Germination under HT by Activating *SOM* Expression

EBS controls primary seed dormancy and interacts genetically with AGL67 in this process (Narro-Diego et al., 2017), raising the question of a potential function for EBS in controlling seed germination under HT. To test this possibility, we first characterized an *ebs* loss-of-function allele, in which the T-DNA was inserted into the first exon and severely suppressed *EBS* transcript accumulation (Supplemental Fig. S7). The *ebs* mutant displayed a higher germination rate than Col-0 specifically under HT. Indeed, *ebs* seeds even germinated at a rate of 10.2% under HT stress at 34°C, a condition that completely abolished seed germination in wild-type Col-0 (Fig. 6A).

Next, we generated *ebs* complementation lines by transforming the *ebs* mutant with a construct driving the expression of *EBS-FLAG* under the control of the *EBS* promoter (*EBSpro*:*EBS-FLAG ebs*, termed *c-EBS*; Supplemental Fig. S7D). As expected, the *EBSpro*:*EBS-FLAG* complementation construct restored *c-EBS* seeds to a wild-type germination rate under HT (Fig. 6A). This result validated our hypothesis that higher germination of the *ebs* mutant under HT was indeed due to the loss of *EBS* function.

Published microarray data demonstrate that *SOM* transcript levels are reduced in the *ebs* mutant (Narro-Diego et al., 2017). To evaluate the effect of EBS on *SOM* expression, we first examined *SOM* expression in wild-type Col-0, *ebs*, and *c-EBS* seeds by RT-qPCR. HT treatment caused an up-regulation of *SOM* transcripts in Col-0 and *c-EBS* seeds but not in *ebs* mutant seeds (Supplemental Fig. S8A), suggesting that *EBS* is required for HT-mediated induction of *SOM* expression. In line with these results, *ebs som* double mutant seeds and *c-EBS som* seeds germinated at the same rate as the *som-2* mutant under HT (Fig. 6B). Furthermore, *ebs*, *som-2*, and *c-EBS som* seeds contained higher GA_4 levels and lower ABA levels than Col-0 or *c-EBS* seeds after exposure to HT stress for 24 h (Supplemental Fig. S8B). We also detected higher GA_1 and GA_3 levels in the seeds of *som-2*, *agl67*, and *ebs* single mutants compared with wild-type Col-0 after HT stress (Supplemental Fig. S8C). These data suggest that EBS controls the thermoinhibition of seed germination by activating *SOM* expression and subsequently altering downstream GA/ABA metabolism.

We next tested whether EBS binds to the *SOM* promoter to induce transcription in hydrated *c-EBS* seeds. ChIP-qPCR revealed that the P3 region within the *SOM* promoter was highly enriched in pull-downs with the anti-FLAG antibody (used to tag EBS) and that HT treatment further enhanced this enrichment (Fig. 6C). The P5 region of the *SOM* promoter and the E1 region (in the exon region) were also enriched, although HT had no additional effect. These data suggest that EBS mainly deposits to the same region as AGL67 in the promoter of *SOM*.

Because EBS is a histone reader that recognizes H3K4me2 or H3K4me3 modifications in vitro (Yang et al., 2018), we next examined whether EBS binding to the *SOM* promoter might depend on the chromatin H3K4 methylation status at the *SOM* locus. To this end, we introduced *c-EBS* into the *atx1-2* (*Arabidopsis homolog of Trithorax*) mutant, which is deficient in H3K4 methyltransferase activity (Alvarez-Venegas et al., 2003), to generate *c-EBS atx1* lines (Supplemental Fig. S9A). ChIP analysis using an anti-H3K4me3 antibody demonstrated that the *atx1-2* mutant had reduced H3K4me3 levels in most *SOM* genomic regions compared with wild-type Col-0, while overexpression of *ATX1-GFP* in the *atx1-2* background (*35Spro*:*ATX1-GFP atx1-2*, abbreviated as *ATX1-GFP/atx1*) increased H3K4me3 levels over the entire *SOM* locus (Supplemental Fig. S9B). Using *ATX1-GFP* seeds, ChIP analysis with an anti-GFP antibody uncovered a strong enrichment at most regions of the *SOM* promoter and exons (Supplemental Fig. S9D). These results suggest that ATX1 targets *SOM* chromatin to mediate H3K4me3 modification at this locus.

Furthermore, EBS enrichment at the *SOM* promoter similarly decreased in *c-EBS atx1* seeds, as measured by ChIP with an anti-FLAG antibody, and did not respond to HT stress either (Supplemental Fig. S9C). We also generated transgenic plants that expressed *ATX1*, cloned in frame with the glucocorticoid receptor gene (*GR*), under the control of the 35S promoter (*35Spro*:*ATX1-GR*, termed as *ATX1-GR*). Dexamethasone (DEX) treatment induces the translocation of ATX1-GR from the cytoplasm to the nucleus to modulate target gene expression (Jing et al., 2019). DEX treatment increased H3K4me3 levels at the *SOM* promoter in *ATX1-GR* seeds as well as *SOM* expression itself (Supplemental Fig. S10, A and B). Phenotype analysis showed that the seed germination rate was relatively higher in *atx1-2*, but lower in the transgenic *ATX-GFP* line, compared with Col-0 under HT stress. Additional DEX also suppressed the seed germination of *ATX-GR* under HT stress (Supplemental Fig. S10C). Together, these data support a model in which EBS reads ATX1-mediated H3K4me3 histone marks at the *SOM* promoter that are required for the activation of *SOM* expression.

To examine whether EBS bridges H3K4me3 modification with histone acetylation for the activation of *SOM* expression after HT, we measured histone acetylation levels for histone H4 at the *SOM* locus in wild-type Col-0 and *ebs* mutant seeds before and after HT stress by ChIP. Only the P3 promoter fragment was enriched with an antibody recognizing acetylated H4K5 (anti-H4K5ac) and further enhanced by HT treatment. However, enrichment at the *SOM* locus was lost in *ebs* mutant seeds (Fig. 6D). These data indicate that EBS reads the H3K4me3 marker at the *SOM* locus and then initiates histone acetylation for increased chromatin accessibility and thus *SOM* expression.

AGL67 Physically Interacts with EBS to Coordinate EBS-Dependent Histone Acetylation at the *SOM* Locus

EBS interacts genetically with AGL67 to regulate seed dormancy (Narro-Diego et al., 2017), indicating that

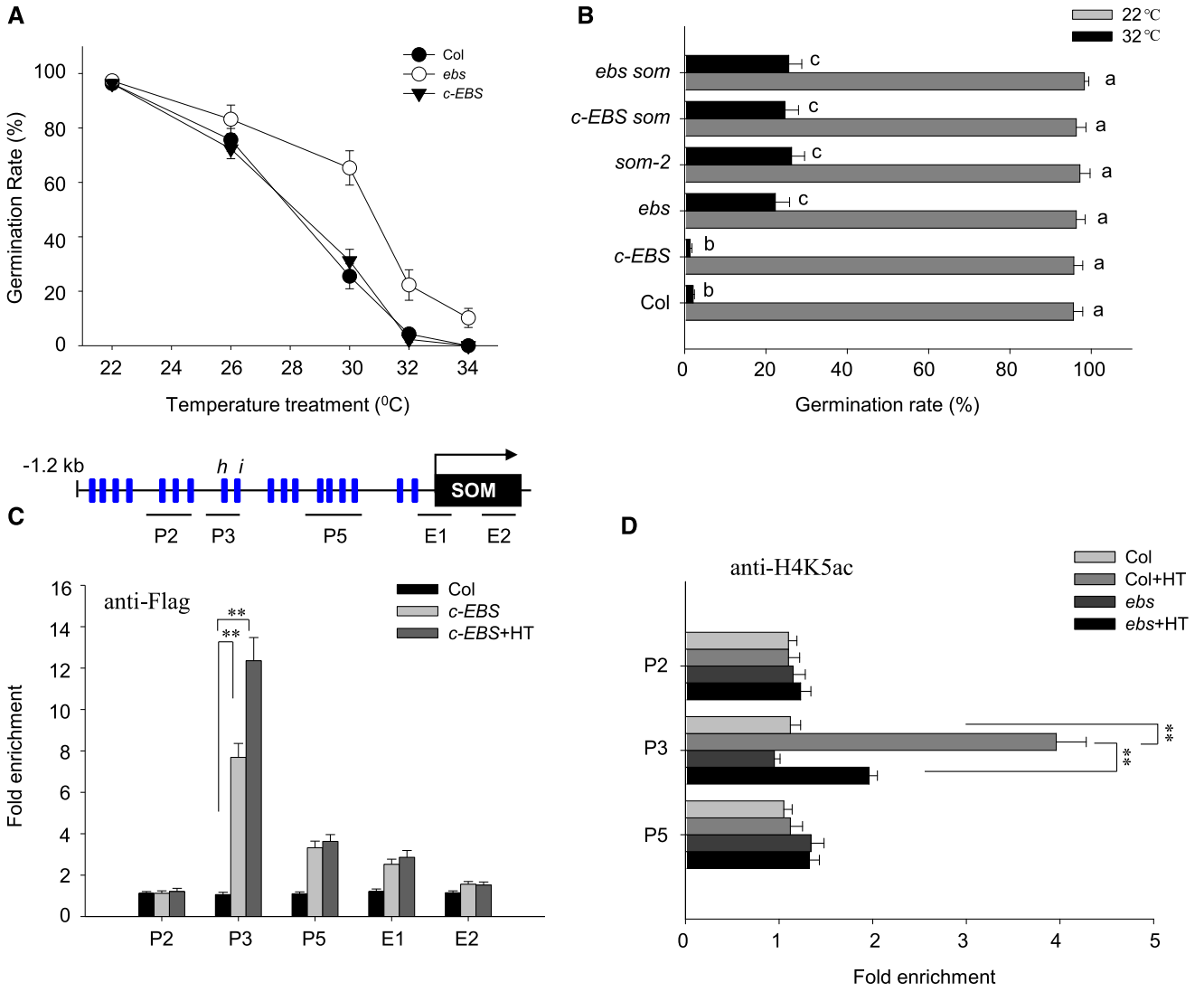

Figure 6. EBS regulates thermoinhibition of seed germination through SOM. A, Hydrated seeds for Col-0, *ebs*, and *c-EBS* were incubated at different temperatures, as indicated, for 5 d, when the germination rate was calculated. Values are means ± SD of three biological replicates. B, Col-0, *som-2*, *ebs*, *c-EBS*, *c-EBS som*, and *ebs som* seeds were incubated at 22°C or 32°C for 5 d, and the germination rate was calculated. Values are means ± SD of three biological replicates; bars labeled with different letters are significantly different at $P < 0.05$ (Tukey's test). C, ChIP-qPCR analysis of the enrichment of EBS at the promoter (P) and exon (E) fragments of the *SOM* locus under normal conditions (22°C) or HT conditions (32°C) for 24 h. Wild-type Col-0 and *c-EBS* seeds were used for the analysis, with an anti-FLAG antibody. Top, Schematic diagram of the *SOM* promoter showing the positions of the CArG-boxes (blue rectangles) and three regions (P2, P3, and P5) covering various cis-elements for ChIP-qPCR amplification; E1 and E2 are located at the beginning and the end of the exon. Bottom, Fold enrichment of five amplified fragments, quantified by qPCR with chromatin isolated from Col-0 and *c-EBS*. *ACTIN2* served as an internal control. Enrichment values were normalized to the level of input DNA. Values are shown as means ± SD from three biological replicates. Asterisks indicate significant difference by Student's *t* test (**$P < 0.01$). D, ChIP-qPCR analysis of histone H4K5 acetylation levels in the promoter and exon fragments of the *SOM* locus in Col-0 or *c-EBS* seeds under normal conditions at 22°C or HT conditions at 32°C for 24 h. An anti-H4K5ac antibody was used for immunoprecipitation. Fold enrichment of five amplified fragments was quantified by qPCR with chromatin isolated from Col-0 and *c-EBS*. *ACTIN2* served as an internal control, and enrichment values were normalized to the level of input H4. Values are shown as means ± SD of three biological replicates. Asterisks indicate significant difference by Student's *t* test (**$P < 0.01$).

EBS and AGL67 function in the same pathway in the context of seed dormancy. To determine whether EBS and AGL67 also work together in response to HT, we introduced *c-EBS* into the *agl67-1* mutant. Seeds from *ebs*, *agl67-1*, and *c-EBS agl67* germinated better than Col-0 seeds under HT, whereas *c-EBS* lines had a germination rate even lower than that of Col-0 seeds (Fig. 7A). In agreement with these observations, HT failed to fully

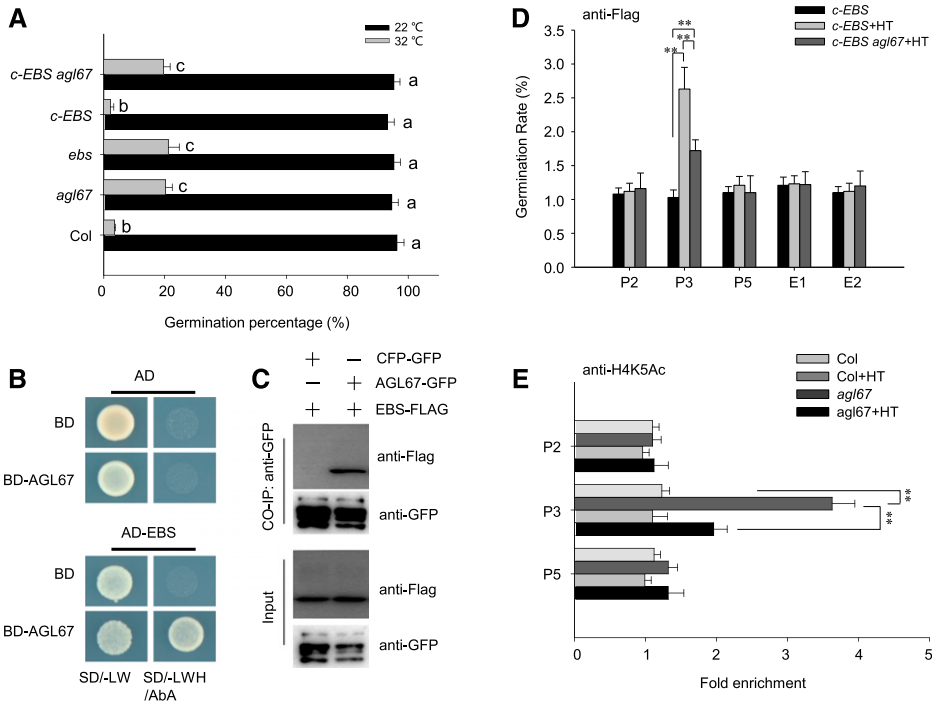

Figure 7. AGL67 interacts with EBS to epigenetically modify H4 acetylation at the *SOM* locus. A, Seed germination rate for Col-0, *agl67*, *ebs*, *c-EBS*, and *c-EBS agl67* incubated under normal conditions at 22°C or HT conditions at 32°C for 5 d, when seed germination rates were recorded. Values are means ± SD of three biological replicates; bars labeled with different letters are significantly different at $P < 0.05$ (Tukey's test). B, Y2H analysis of the interaction between EBS and AGL67. Yeast cells cotransformed with the indicated constructs were grown on SD medium lacking Trp/Leu (-LW) or Trp/Leu/His (-LWH) with 100 ng mL^{-1} aureobasidin A (AbA). AD, DNA-activation domain of GAL4; BD, DNA-binding domain of GAL4. C, CoIP assay showing the interaction between EBS and AGL67. Total protein (input) was extracted from hydrated seeds of *AGL67-GFP EBS-FLAG* and immunoprecipitated with GFP-Trap resin. Total protein extract from *CFP-GFP SOM-FLAG* was used as a negative control. Total and immunoprecipitated proteins were analyzed using anti-GFP or anti-FLAG antibodies. These experiments were repeated three times, with similar results. D, ChIP-qPCR analysis of the enrichment of EBS in the promoter (P) and exon (E) fragments of the *SOM* locus under normal conditions at 22°C or HT conditions at 32°C for 24 h. Seeds from *c-EBS* or *c-EBS agl67* were used for analysis. An anti-FLAG antibody was used for immunoprecipitation. *ACTIN2* served as an internal control, and enrichment values were normalized to the level of input DNA. Values are shown as means ± SD of three biological replicates. E, ChIP-PCR analysis of H4K5ac at the *SOM* promoter in Col-0 and *agl67* under normal conditions (22°C) or HT (32°C) for 24 h. *ACTIN2* served as an internal control, and enrichment values were normalized to the level of input histone H4. Values are shown as means ± SD of three biological replicates. Asterisks indicate significant difference by Student's *t* test (**$P < 0.01$).

induce *SOM* expression in *agl67-1*, *ebs*, and *c-EBS agl67* seeds (Supplemental Fig. S11). These results are consistent with AGL67 being required for EBS-mediated *SOM* expression under HT treatment. Furthermore, EBS and AGL67 physically interact, as evidenced in a Y2H assay (Fig. 7, B and C). EBS-FLAG coimmunoprecipitated with AGL67-GFP in a Co-IP using an anti-GFP antibody and total protein extracts from hydrated *AGL67-GFP EBS-FLAG* seeds (Fig. 7C), further confirming that EBS and AGL67 interact in planta.

To explore whether AGL67 recruits EBS to the *SOM* promoter and thereby mediates histone acetylation, we examined the binding of EBS at the *SOM* locus in hydrated *c-EBS* or *c-EBS agl67* seeds. ChIP-qPCR exposed the enhanced binding of EBS to the P3 fragment of the *SOM* promoter in response to HT treatment for 24 h, which was partially counteracted by the loss of *AGL67* function in *c-EBS agl67-1* seeds (Fig. 7D). These data indicate that AGL67 facilitates EBS binding to the *SOM* promoter upon exposure to HT stress.

In agreement with this conclusion, ChIP-PCR analysis showed that HT treatment increased H4K5ac levels at the P3 fragment within the *SOM* locus, but this was abolished in the *agl67-1* mutant (Fig. 7E). These data are consistent with the model from our genetic analysis: AGL67 and EBS promote *SOM* expression. They further establish that AGL67 recruits EBS to enhance H4 acetylation levels at the *SOM* locus to induce *SOM* expression, which results in thermoinhibition of seed germination. EBS function may require HISTONE ACETYLTRANSFERASE OF THE MYST FAMILY (HAM) members HAM1 and HAM2, previously reported to be recruited by the histone mark reader MORF RELATED GENEs MRG1 and MRG2 for H4K5 acetylation modification (Xu et al., 2014b).

DISCUSSION

AGL67 Controls Seed Germination Thermotolerance through SOM

We had previously shown that the negative regulator of ABA signaling, AFP2, influences the trans-activation activity of ABI5 for *SOM* expression, thereby enhancing thermotolerance of seed germination (Chang et al., 2018). In this study, we identified a 2.4-kb fragment upstream of the *SOM* start codon that was sufficient to drive *SOM* expression under HT (Fig. 1C) and fully rescued the *som* mutant phenotype (Fig. 1, A and B). We then demonstrated that SOM can bind to its own promoter and activate its own expression (Fig. 1, D and E). Zinc-finger proteins (of which SOM is one) stabilize RNA by binding to A/U-rich 3′ untranslated regions (Laity et al., 2001; Jang, 2016); the *SOM* promoter is A/T rich and therefore constitutes a likely target for SOM binding. This strategy may allow *SOM* to quickly drive the accumulation of its own encoded protein and thus enact its biological function, as for example in response to HT stress. Indeed, other regulatory factors involved in salicylic acid, ABA, or light signaling, such as NONEXPRESSER OF PR GENES1, ABI5, and ELONGATED HYPOCOTYL5, bind to their own promoters for feedback activation of their own expression (Abbas et al., 2014; Xu et al., 2014a; Chen et al., 2019b).

Previous data showed that ABI3 interacts with ABI5 and DELLAs to form a complex that binds to the RY motifs in the *SOM* promoter and control its expression under HT stress (Lim et al., 2013). Here, we identified the MADS-box transcription factor AGL67 as an important player that associates with the *SOM* promoter (Fig. 3; Supplemental Fig. S2). AGL67 was reported to be an important regulator of seed desiccation tolerance: overexpressing AGL67 partially rescued the low germination rate of the strong (and desiccation-sensitive) allele *abi3-5* after dry treatment during seed storage (González-Morales et al., 2016). AGL67 also regulates primary seed dormancy (Narro-Diego et al., 2017).

In this study, we report that *agl67* mutant seeds have a higher germination rate, whereas *AGL67*-overexpressing seeds have a lower germination rate, when compared with Col-0 seeds after HT stress (Fig. 5A). These results suggest that AGL67 negatively controls seed germination under HT. Genetic analysis further confirmed that *SOM* is epistatic to *AGL67* in thermoinhibition of seed germination, because both *AGL67-ox som* and *agl67 som* seeds showed a higher germination rate that was similar to that of the *som-2* mutant (Fig. 5B). GUS staining in *SOMpro:GUS* lines and RT-qPCR and transient transformation analyses further revealed that AGL67 transactivates *SOM* expression (Figs. 2 and 3). In particular, EMSA and ChIP analysis demonstrated that AGL67 specifically binds to the proximal region of the *SOM* promoter to activate its expression by recognizing the cis-*j* and cis-*k* elements containing CArG motifs. Deleting this motif compromised AGL67-mediated activation of *SOM* expression (Fig. 3, C and D).

Not only do AGL67 and SOM bind to the *SOM* promoter, but they also colocalized to the nucleus (Fig. 4, E and F). Furthermore, ChIP analysis showed that both of AGL67 and SOM bind to the same P3 region within the *SOM* promoter (Figs. 1E and 3A). Their interaction was confirmed by Y2H assay, in vitro pull-down, in vivo BiFC, and Co-IP experiments (Fig. 4). Transient transfection of protoplasts demonstrated that expressing SOM enhanced the activation conferred by AGL67 on *SOM* expression (Fig. 3, C and D). Based on these data, we hypothesize that the interaction of SOM and AGL67 intensifies the trans-activation activity of AGL67 at the *SOM* promoter under HT.

AGL67 Recruits the Histone Reader EBS to Epigenetically Activate *SOM* for Thermoinhibition of Seed Germination

In a previous study, EBS was shown to mediate the break of seed primary dormancy; *SOM* expression was also lower in the *ebs* mutant based on microarray analysis (Narro-Diego et al., 2017), consistent with a role for EBS in controlling seed germination through SOM. In support of this hypothesis, we established that both *ebs* and *som-2* mutants shared a high germination rate after HT stress, in contrast to wild-type Col-0 seeds (Fig. 6, A and B). *SOM* transcript levels remained low in *ebs* mutant seeds after HT stress, but this was fully complemented by introducing the *EBSpro:EBS-FLAG* construct (expressing *EBS-FLAG* from the *EBS* promoter) into the *ebs* mutant background (Fig. 6A), suggesting that EBS positively regulates *SOM* expression after HT stress. Seeds of both the *ebs som* double mutant and the *c-EBS som* line displayed higher germination rates than Col-0 seeds (Fig. 6B). As a result, EBS controls seed germination through activating *SOM* expression and thus altering downstream ABA/GA metabolism (Supplemental Fig. S8).

EBS was reported to act as a bivalent histone mark reader via its BAH domain, which recognizes trimethylated Lys-27 of histone H3 (H3K27me3), as well as via the PHD, itself recognizing trimethylation of Lys-4 (H3K4me3; Yang et al., 2018). In yeast and animals, proteins with PHDs bind to H3K4me3 and act as a molecular bridge between local changes in histone acetylation or methylation levels and activation of gene expression (Wysocka et al., 2006). In Arabidopsis, ORIGIN OF REPLICATION COMPLEX1 is a PHD that specifically binds to H3K4me3 to stimulate target gene expression by increasing histone H4 acetylation and H4K20 trimethylation (de la Paz Sanchez and Gutierrez, 2009). EBS exhibits a higher affinity for H3K27me3 than H3K4me3; however, removing the C-terminal extension of EBS increased its affinity for H3K4me3 (Yang et al., 2018).

In this study, we show that EBS specifically binds to the *SOM* promoter within the P3 region, containing functional *cis-j/k* CArG-box elements (Fig. 6C). The recruitment of EBS to the *SOM* promoter depends on ATX1-mediated trimethylation at H3K4 (Supplemental

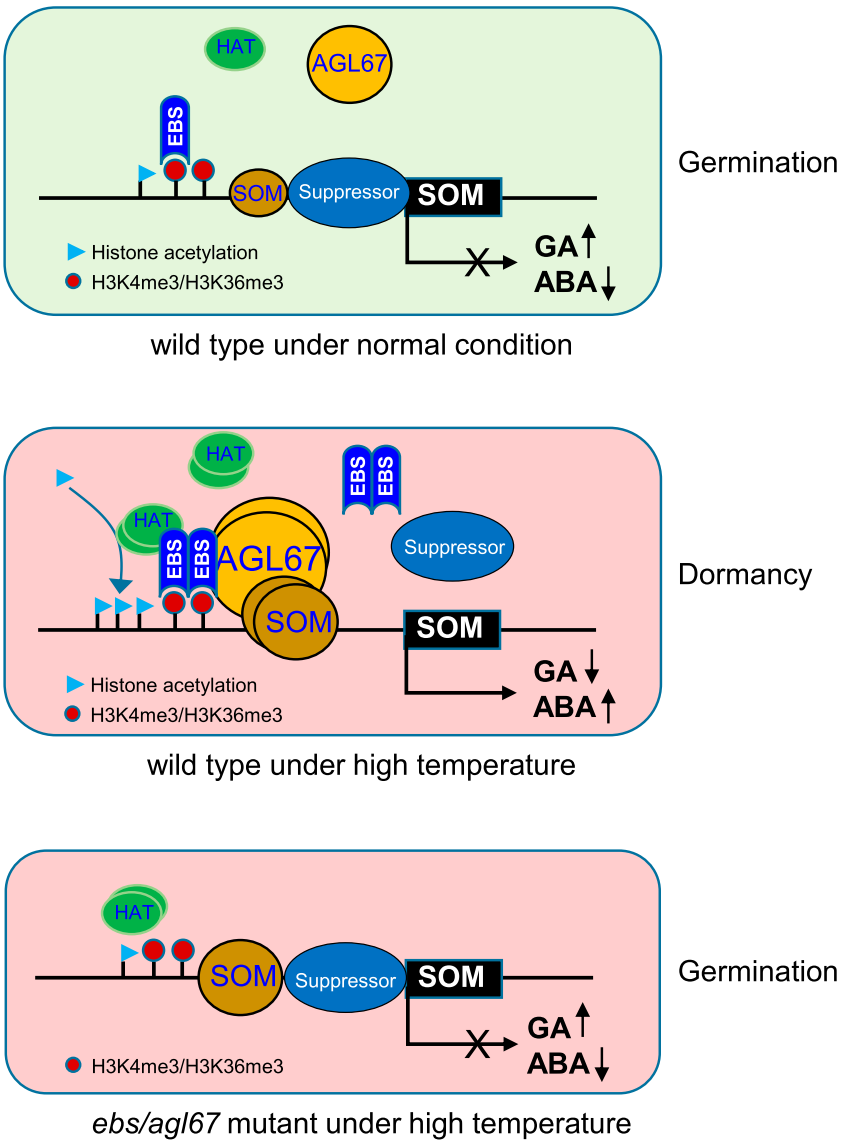

Figure 8. Proposed model for the control of *SOM* expression and thermoinhibition of seed germination by AGL67 and EBS through epigenetic increase of histone acetylation levels. Under normal conditions, low levels of AGL67 and EBS cannot induce *SOM* expression because of the presence of a repressor complex at the *SOM* promoter, which maintains high GA and low ABA levels compatible with seed germination. However, HT treatment induces the accumulation of AGL67, which physically interacts with EBS at the *SOM* locus to epigenetically increase H4K5ac levels through the recruitment of histone acetyltransferases (HATs) to the *SOM* promoter. The subsequent increase in *SOM* transcription leads to altered GA/ABA metabolism that suppresses seed germination under HT. However, in *agl67* or *ebs* mutant seeds, *SOM* cannot be induced due to the loss of AGL67 or EBS at the *SOM* promoter, which leaves the repressor free to occupy the *SOM* promoter and again block *SOM* expression, ultimately driving the higher germination rates under HT seen in *som*, *ebs*, and *agl67* mutants.

Fig. S9). Histone marker readers, such as MRG1/2, bind to H3K4 or H3K36me3 via their chromodomains and recruit H4-specific acetyltransferases, such as HAM1 and HAM2, which catalyze H4K5 acetylation and promote target gene expression (Xu et al., 2014b). Other proteins, such as CONSTANS or PIF7, have been shown to interact with MRG1/2 and modulate their recognition of H3K4me3 or H3K36me3 around target genes, ultimately controlling plant photoperiodic flowering (for CONSTANS) or plant shade avoidance (for PIF7; Bu et al., 2014; Peng et al., 2018). As is the case for MRG1/2, EBS bridges H3K4me3 and H4K5 acetylation for transcriptional activation of *SOM* during HT stress based on the observation that the *ebs* mutation reduced the positive effect of HT on H4K5 acetylation at the *SOM* locus (Fig. 6D). EBS and its putative paralog SHORTLIFE read H3K27me3 H3 histone marks through the BAH domain to form a complex with EMBRYONIC FLOWER1 (EMF1) and play a Polycomb Repressive Complex1-like repressive role (Li et al., 2018). Furthermore, the EMF1 complex interacts with the MADS-box transcription factors FLOWERING LOCUS C and FLOWERING LOCUS M to suppress *FLOWERING LOCUS T* expression and prevent flowering (Wang et al., 2014). Our Y2H and Co-IP results show that the MADS-box protein AGL67 also interacts with EBS (Fig. 7, B and C). The germination rate of *ebs* or *agl67* under HT stress was clearly higher than that of Col-0 or *c-EBS* seeds. In addition, the introduction of *c-EBS* into the *agl67-1* background resulted in the same germination rate as the *agl67-1* mutant under HT stress (Fig. 7A) and was accompanied by lower *SOM* expression under HT stress (Supplemental Fig. S10). These data suggest that EBS depends on AGL67 to activate *SOM* expression under HT.

In agreement with our findings, *AGL67* and *SOM* expression was low in freshly harvested *ebs* mutant seeds, as determined by a microarray analysis (Narro-Diego et al.,

2017). We note that HT treatment increased the affinity of EBS to the P3 region in the *SOM* promoter in Col-0 seeds but not in *agl67* mutant seeds (Fig. 7D), suggesting that EBS requires AGL67 to bind to the *SOM* P3 promoter region. It is possible that HT increases the transcription rate of *AGL67* (Supplemental Fig. S5A), thereby recruiting more EBS to H3K4me3 marks at the *SOM* promoter and ultimately initiating H4K5 acetylation and opening the chromatin at the *SOM* locus. In support of this hypothesis, HT stress did not increase H4K5 acetylation at the *SOM* locus in *agl67* mutant seeds (Fig. 7E) and resulted in lower *SOM* expression (Supplemental Fig. S11). Because HTs increased the protein level of SOM, our data also showed that SOM synergistically enhances the trans-activation effect of AGL67 on *SOM* expression (Fig. 3D). It is possible that the interaction of SOM and AGL67 collaboratively intensifies the recruitment of EBS to the *SOM* promoter, ensuring rapid activation of *SOM* expression following exposure to HT stress. Thus, the SOM-AGL67-EBS module forms a positive feedback loop that efficiently and rapidly magnifies the inhibitory effect of SOM on seed germination, guaranteeing seed dormancy under harsh HT conditions. Future research should compare the effect of SOM on the deposition of EBS to the *SOM* promoter between Col and *som-2* mutant seeds.

In summary, our study uncovers a mechanism that couples a transcription factor, a reader of histone methylation, and chromatin structure reprogramming through histone acetylation during thermoinhibition of seed germination (Fig. 8). Under normal conditions, low levels of SOM and AGL67 cannot induce *SOM* expression due to the presence of a suppressor complex such as PWR at the *SOM* locus (Yang et al., 2019). Under these conditions, seeds accumulate more GA and less ABA, ensuring seed germination. When subjected to thermoinhibitory temperatures, HT induces the accumulation of AGL67, which interacts with and recruits EBS to the *SOM* promoter by reading H3K4me3 marks. Subsequently, H4K5 at the *SOM* locus is acetylated, which activates *SOM* expression and ultimately up-regulates ABA biosynthesis and GA degradation, inhibiting seed germination. Concurrently, the interaction of SOM and AGL67 reinforces the trans-activation effect of AGL67, possibly preventing a suppressor complex from binding to the *SOM* promoter. However, inactivation of AGL67 or EBS decreases the extent of histone acetylation, allowing the suppressor complex to move back onto the promoter, thus silencing *SOM* expression during seed germination under HT. Together, our findings reveal AGL67 as an important regulator of the thermoinhibition of seed germination and highlight the critical role of EBS in linking H3K4 methylation reading and H4K5 acetylation modifications to the activation of SOM in response to HT.

MATERIALS AND METHODS

Plant Materials and Growth Conditions

All Arabidopsis (*Arabidopsis thaliana*) T-DNA insertion mutants, including *agl67-1* (SAIL_124_F12), *agl67-2* (SALK-144818), *ebs* (CS906904), and *atx1-2* (SALK_149002), were obtained from the Arabidopsis Biological Resource Center. *som-2* was generously provided by Giltsu Choi. *ATX1-GFP* and *ATX1-GR* were reported previously (Jing et al., 2019). Double mutants or lines carrying two different transgenes were generated by crossing individual lines and selecting homozygous progeny. Seeds were surface sterilized and sown on 0.8% (w/v) agar (pH 5.7) plates under white light (50 μmol m^{-2} s^{-1}). Adult plants were grown in soil with vermiculite (3:1) at 22°C under long-day (16 h of light/8 h of darkness) conditions for 6 to 8 weeks, and seeds were harvested at the same time in each batch for germination or dormancy assays.

Plasmid Construction and Transgenic Plants

To generate the *SOM-FLAG* construct, the 2-kb promoter fragment upstream of the start codon was fused with the *SOM* coding region by PCR amplification with PrimeSTAR enzyme (Takara) and cloned into the pRI101-6FLAG vector by replacing the *35Spro* fragment with the resulting PCR product. Similarly, a genomic fragment containing an approximately 1-kb upstream region and the coding region of *EBS* was PCR amplified and cloned into the pRI101-6Flag vector, removing the *35Spro* fragment to generate the *EBSpro:EBS-FLAG* construct. To generate the *35Spro:AGL67-FLAG* construct, the coding region of *AGL67* was inserted at the *Nde*I/*Sal*I sites of the pRI101-6FLAG vector and placed under the control of the 35S promoter. The 2.4-kb *SOM* promoter fragment was also inserted at the *Hin*dIII/*Bam*HI sites of pBI101 to generate the *SOMpro:GUS* reporter. These constructs were introduced into Arabidopsis Col-0 plants by *Agrobacterium tumefaciens*-mediated transformation (Clough and Bent, 1998). Primers used for cloning are listed in Supplemental Table S1.

Seed Germination Assays

Seeds were harvested and dried for 3 to 5 weeks at room temperature, and seed germination assays were performed as previously described (Chen et al., 2019a; Yang et al., 2019). In brief, seeds were surface sterilized in a 5% (v/v) hypochlorite and 0.02% (v/v) Triton X-100 solution for about 10 min and then rinsed several times with sterile water before being plated on germination medium consisting of one-half-strength Murashige and Skoog salts with 1% (w/v) Suc. After stratification at 4°C for 3 d, plates were placed in constant light to initiate germination, at a constant temperature (22°C as the control, 32°C for HT stress, or different ambient temperatures as indicated) for 5 d. A seed was considered to have germinated when its radicle protruded from the seed coat. For each germination assay, at least three biological replicate experiments were performed.

Protein Extraction and Immunoblots

We extracted total protein from hydrated seeds using extraction buffer (50 mM Tris-HCl, pH 7.5, 150 mM NaCl, 1 mM EDTA, pH 8, 0.1% [v/v] Triton X-100, 10 mM NaF, and 5% [v/v] glycerol) supplemented with phosphatase inhibitor cocktail (Roche) and 1 mM phenylmethylsulfonyl fluoride (Sigma-Aldrich). Proteins were cleared by centrifugation at 15,000*g* for 10 min at 4°C. Protein concentration was measured using Bradford Quantitative Reagent (Invitrogen). The extracted protein (15-μg aliquot) was separated by electrophoresis on a 12% SDS-polyacrylamide gel and blotted onto polyvinylidene difluoride membranes, which were then probed with the appropriate primary anti-FLAG (1:3,000; Sigma-Aldrich), anti-GFP (1:3,000; Clontech), or anti-actin (1:1,000; Sigma-Aldrich) antibody and horseradish peroxidase-conjugated goat anti-mouse secondary antibody (1:3,000; Promega). Signals were detected using a ONE-HOUR IP-Western Kit (Genescript).

Y1H and Y2H Assays

The Matchmaker Gold Y1H Library Screening system (Clontech) was used for Y1H and Y2H assays. The construct carrying the 2-kb *SOM* promoter fragment was linearized, and the bait-reporter yeast (*Saccharomyces cerevisiae*) strain was obtained by integrating the linearized construct into the Y1HGold strain genome. The cDNA library was constructed with mRNAs isolated from wild-type hydrated seeds. The bait-reporter strain and cDNA library were used to screen for putative SOM regulators. Positive colonies were isolated on selective medium (synthetic dextrose/-Leu) with 100 ng mL^{-1} aureobasidin A. Positive prey fragments were identified by PCR and DNA sequencing and BLAST.

For the Y2H assay, the full-length cDNAs of *AGL67*, *SOM*, and *EBS* were cloned into the pGBKT7 bait vector and the pGADT7 prey vector using the

In-Fusion cloning system (Clontech). Two-hybrid screening was performed using the mating proto-Col-0 described in the Matchmaker Gold Yeast Two-Hybrid user manual (Clontech).

In Vitro Pull-Down Assays

The coding regions for *AGL67* and *SOM* were cloned into the pGEX-4T-1 (Pharmacia) and pET28a (Merck) vectors to generate the pGST-AGL67 and pHis-SOM constructs, respectively. The primers used for construction are listed in Supplemental Table S1. For prokaryotic protein expression, the constructs were transformed into the *Escherichia coli* Rosetta strain, and protein accumulation was induced by isopropyl β-D-1-thiogalactopyranoside. Soluble GST-AGL67 protein was extracted and immobilized onto Glutathione Sepharose beads (GE Healthcare), while the soluble His-SOM was extracted and immobilized onto Ni-NTA agarose beads (Qiagen). For pull-down assays, 2 μg of His-SOM was incubated with GST alone or GST-AGL67 in binding buffer (50 mM Tris-HCl, pH 8, 100 mM NaCl, and 1 mM EDTA) at 4°C overnight. Pulled-down proteins were extensively washed with buffer (50 mM Tris-HCl, pH 7.4, 100 mM NaCl, and 0.6% [v/v] Triton X-100) before the samples were resolved on 8% SDS-PAGE gels and analyzed by immunoblot analysis using anti-His antibody (Abmart) or anti-GST antibody (Abmart) followed by a mouse secondary antibody (1:5,000; Promega).

CoIP

Plants containing the transgenes *AGL67-GFP* and *SOM-FLAG* or *AGL67-GFP* and *EBS-FLAG* were generated by crossing *AGL67-GFP* with *SOM-FLAG* or *EBS-FLAG*, respectively. We also crossed a line expressing *GFP* to *SOM-FLAG* and a line expressing a *CFP-GFP* fusion to *EBS-FLAG* to generate suitable negative control genotypes. For the in vivo Co-IP using AGL67-GFP as bait, hydrated *AGL67-GFP SOM-FLAG* or *AGL67-GFP EBS-FLAG* transgenic seeds were ground to a fine powder in liquid nitrogen. Total proteins were extracted in MOPS buffer (100 mM MOPS, pH 7.6, 150 mM NaCl, 0.1% [w/v] Nonidet P-40, 1% [v/v] Triton X-100, 20 mM iodoacetamide, 1 mM phenylmethylsulfonyl fluoride, 2 μg L^{-1} aprotinin, 5 μg L^{-1} leupeptin, 1 μg L^{-1} pepstatin, 2× Complete Protease Inhibitor Cocktail, and PhosStop Cocktail from Roche), centrifuged at 13,000 rpm at 4°C for 10 min, and filtered through two layers of Miracloth. Supernatant (1 mL) was incubated with GFP-Trap (Chromotek) overnight under gentle rotation at 4°C. Beads were washed four times with wash buffer (50 mM Tris, pH 8, 150 mM NaCl, and 0.1% [v/v] Triton X-100), and the proteins were eluted at 95°C for 10 min in 2× loading buffer (100 mM Tris-HCl, pH 6.8, 200 mM DTT, 2% [w/v] SDS, 20% [v/v] glycerol, and 0.2% [w/v] Bromophenol Blue) and analyzed by immunoblotting with anti-FLAG (1:3,000; Sigma-Aldrich) or anti-GFP (1:3,000; Clontech) monoclonal antibodies.

EMSA

EMSA was performed as previously described (Hu et al., 2014). Briefly, oligonucleotide probes were synthesized, annealed, and labeled using the Biotin-DNA labeling kit (Pierce). *E. coli* BL21 cells that had been transformed with pGST-AGL67 were induced with the addition of 0.5 mM isopropyl β-D-1-thiogalactopyranoside at 16°C when the OD_{600} reached 1.5. Cells were lysed in lysate buffer (50 mM Tris-HCl, pH 8, 1 mM EDTA, and 100 mM NaCl) with an ultrasonic cell crusher. After centrifugation at 13,000 rpm at 4°C for 15 min, the supernatant was purified by GST resin affinity chromatography (Invitrogen). The oligonucleotide probes containing the wild-type or mutated CArG motif were labeled with biotin and synthesized from Generay Biotech. Oligonucleotides were diluted to 10 μM, heated to 95°C for 5 min, and slowly cooled to room temperature. Briefly, 1 pmol of labeled probe or cold probe was incubated with 0.1 μg of the indicated protein in 20 μL of reaction buffer (25 mM HEPES, pH 8, 40 mM KCl, 5 mM $MgCl_2$, 1 mM DTT, 1 mM EDTA, 8% [v/v] glycerol, and 1 μg of poly[dI-dC]) for 20 min at room temperature. Then, 5 μL of 5× loading buffer (12.5% [w/v] Ficoll-400, 0.2% [w/v] Bromophenol Blue, and 0.2% [w/v] xylene cyanol FF) was added to the reaction mixture and loaded onto a 4.5% polyacrylamide gel in 0.5× Tris-borate/EDTA. The chemiluminescence of biotin-labeled DNA was detected using the Light Shift Chemiluminescent EMSA Kit (Pierce).

ChIP-qPCR Analysis

Chromatin affinity purification was performed as described previously (Hu et al., 2014). Seeds were cross-linked with a 1% (v/v) formaldehyde solution under a vacuum for 1 h. The chromatin was extracted and sheared to an average length of 300 to 500 bp by sonication and then immunoprecipitated with specific antibodies, including anti-GFP (catalog no. 6795; Sigma-Aldrich), anti-FLAG M2 gel (catalog no. A2220; Sigma-Aldrich), anti-histone H4 (catalog no. 04-858; Millipore), and anti-acetyl-histone H4K5 (catalog no. 07-327; Millipore). The cross-linking was then reversed, and the amount of each immunoprecipitated DNA fragment was determined by qPCR using gene-specific primers (Supplemental Table S1).

BiFC Analysis

The coding regions of *AGL67* and *SOM* were cloned into pGreen binary vectors to add each half of the *YFP* coding sequence (*nYFP* and *cYFP*) upstream of and in frame with *AGL7* or *SOM*, to generate *nYFP-AGL67* and *cYFP-SOM*. Combinations of *nYFP-AGL67/cYFP-SOM*, *nYFP-AGL67/nYFP*, and *cYFP/cYFP-SOM* were coinfiltrated into *Nicotiana benthamiana* leaves by *A. tumefaciens*-mediated transient transfection. After 48 h, YFP fluorescence in *N. benthamiana* leaf cells was observed with a Zeiss LSM710 confocal microscope as described previously (Hu et al., 2014).

RT-qPCR Analysis

Total RNA was extracted from hydrated seeds using TRIzol reagent (Invitrogen). RT-qPCR was performed as described (Hu et al., 2014). Briefly, first-strand cDNA was synthesized from 1.5 μg of DNase-treated RNA in a 20-μL reaction volume using Moloney murine leukemia virus reverse transcriptase (Fermentas) with oligo(dT)18 primer. The cDNA samples were diluted to 2 to 10 ng mL^{-1}, and qPCR was performed in the presence of SYBR Green I Master Mix on a Roche LightCycler 480 real-time PCR machine according to the manufacturer's instructions. All RT-qPCR experiments were independently performed in triplicate, and representative results are shown. *PP2A* was used as an internal control. The primer pairs for RT-qPCR are listed in Supplemental Table S1.

Protoplast Transient Expression Assay

For the transient expression assay, a 2.4-kb *SOM* promoter fragment was inserted into the pGreenII 0800-LUC vector to generate a series of *SOMpro:LUC* reporter constructs. The coding sequences of *AGL67* and *SOM* were inserted into the pGreenII 62-SK vector and placed under the control of the 35S promoter. For analysis of the truncated *SOM* promoter activity, the corresponding CArG-box in the *SOM* promoter was simultaneously removed to generate different *SOM* promoter variants (*pC-SOMΔP3* and *pC-SOMΔP4*), as described in the text. The variants of the *SOM* promoter were also inserted into the pGreenII 0800-LUC vector to generate the reporter constructs. All primers used for these constructs are listed in Supplemental Table S1. After protoplast preparation and subsequent transfection, firefly luciferase and renilla luciferase activities were measured using the Dual-Luciferase Reporter Assay System (Promega), and the LUC/REN ratio was presented.

GA_4 and ABA Content Measurement

The GA and ABA contents of hydrated seeds were determined as previously described (Yang et al., 2019). In brief, hydrated and stratified seeds were incubated at 22°C or 32°C for 24 h before phytohormone analysis. For GA content analysis, seeds were weighed and ground to a fine powder in liquid nitrogen. Internal standards of 1 ng g^{-1} [$^2H_2$]GA_4 were added to the samples prior to extraction with 500 μL of solvent (methanol:water, 80:20, v/v) at 4°C for 12 h. The supernatants were sequentially passed through preconditioned tandem solid-phase extraction cartridges containing C18 adsorbent (50 mg) and a strong anion-exchange adsorbent (200 mg). The strong anion-exchange cartridge was then rinsed with 2 mL of 20% (v/v) methanol, and the targeted acidic phytohormones were eluted with 3 mL of acetonitrile with 1% (v/v) formic acid. The eluent was evaporated under a mild liquid nitrogen stream at 35°C and redissolved in 100 μL of water. The solution was acidified with 10 μL of formic acid and extracted with 1 mL of ether twice. The combined ether phase was dried under nitrogen gas and reconstituted in 100 μL of acetonitrile followed by the addition of 10 μL of triethylamine (20 mmol mL^{-1}) and 10 μL of 3-bromoactonyltrimethylammonium bromide (20 μmol mL^{-1}). The reaction solution was vortexed at 35°C for 30 min and then evaporated under nitrogen gas. The samples were dissolved in 200 μL of 10% (v/v) acetonitrile and subjected to nano-liquid chromatography-electrospray ionization-quadrupole time-of-flight-mass spectrometry analysis.

For ABA measurement, seeds were ground in liquid nitrogen, and 45 pmol of [$^2H_2$]ABA internal standard was added to 200 mg of powder. The samples were extracted with 2 mL of methanol at 20°C overnight. After centrifugation at 4°C for 15 min at 18,000 rpm, the supernatant was dried under nitrogen gas and dissolved in 1 mL of 5% (v/v) ammonia solution. Crude extracts were purified on a preconditioned Oasis MAX strong anion-exchange column (Waters), and the samples were eluted with 4 mL of methanol containing 5% (v/v) formic acid. The eluent was dried under nitrogen gas and dissolved in 200 μL of 80% (v/v) methanol and then subjected to ultra-performance liquid chromatography-tandem mass spectrometry analysis.

GUS Staining

Seeds from different genetic backgrounds and homozygous for the *SOMpro:GUS* reporter were hydrated in water for 3 h and then plated on 0.8% (w/v) agar (pH 5.7) for 24 h at normal conditions (22°C) or HT (32°C). After heat treatment, seeds were incubated in 0.1 M sodium phosphate buffer containing 50 mM $K_3Fe(CN)_6$, 50 mM $K_4Fe(CN)_6$, and 1 mM 5-bromo-4-chloro-3-indolyl-β-D-glucuronide at 37°C for 12 h. GUS staining was examined with a stereomicroscope, and images were captured with a digital camera (Zeiss).

Accession Numbers

Sequence data from this article can be found in the GenBank/EMBL data libraries under the following accession numbers: ABA1, AT5G67030; ATX1, AT2G31650; AGL67, AT1G77950; CYP707A2, AT2G29090; EBS, AT4G22140; NCED6, AT3G24220; GA2ox2, AT1G30040; GA3ox1, AT1G15550; GA3ox2, AT1G80340; and SOM, AT1G03790.

Supplemental Data

The following supplemental materials are available.

Supplemental Figure S1. Validation of *SOM-FLAG*, *35Spro:SOM-GFP*, and *35Spro:AGL67-FLAG* by immunoblot analysis.

Supplemental Figure S2. AGL67 binds to the *SOM* promoter in a Y1H analysis.

Supplemental Figure S3. Expression pattern of AGL67 in different tissues or developmental stages.

Supplemental Figure S4. Identification of T-DNA insertion mutants in *AGL67*.

Supplemental Figure S5. Genotype analysis of the crossed lines of *agl67* and *SOM-GFP*.

Supplemental Figure S6. HT regulates transcript levels of GA and ABA metabolic genes.

Supplemental Figure S7. Identification of a T-DNA insertion mutant of *EBS*.

Supplemental Figure S8. EBS regulates *SOM* expression and alters downstream GA/ABA levels.

Supplemental Figure S9. ATX1 influences the binding of EBS to the *SOM* promoter.

Supplemental Figure S10. ATX1 mediates the HT-induced increase of H3K4me3 level at the *SOM* locus, thus activating *SOM* expression to suppress seed germination.

Supplemental Figure S11. *SOM* transcript levels in Col-0, *c-EBS*, and *ebs* mutant seeds before and after HT stress.

Supplemental Table S1. List of primers used in this study.

Supplemental Data Set S1. Sequence information of the *SOM* promoter and its truncated versions.

ACKNOWLEDGMENTS

We thank Giltsu Choi (Department of Biological Sciences, Korea Advanced Institute of Science and Technology, Korea) and the Arabidopsis Biological Resource Center for kindly providing mutant seeds. We also thank Plant Editors (planteditors.com) and Kathleen Farquharson (University of Washington) for English polishing.

Received January 17, 2020; accepted June 10, 2020; published June 23, 2020.

LITERATURE CITED

Abbas N, Maurya JP, Senapati D, Gangappa SN, Chattopadhyay S (2014) Arabidopsis CAM7 and HY5 physically interact and directly bind to the HY5 promoter to regulate its expression and thereby promote photomorphogenesis. Plant Cell **26:** 1036–1052

Alvarez-Venegas R, Pien S, Sadder M, Witmer X, Grossniklaus U, Avramova Z (2003) ATX-1, an Arabidopsis homolog of trithorax, activates flower homeotic genes. Curr Biol **13:** 627–637

Argyris J, Dahal P, Hayashi E, Still DW, Bradford KJ (2008) Genetic variation for lettuce seed thermoinhibition is associated with temperature-sensitive expression of abscisic acid, gibberellin, and ethylene biosynthesis, metabolism, and response genes. Plant Physiol **148:** 926–947

Auge GA, Blair LK, Burghardt LT, Coughlan J, Edwards B, Leverett LD, Donohue K (2015) Secondary dormancy dynamics depends on primary dormancy status in *Arabidopsis thaliana*. Seed Sci Res **25:** 230–246

Bu Z, Yu Y, Li Z, Liu Y, Jiang W, Huang Y, Dong AW (2014) Regulation of Arabidopsis flowering by the histone mark readers MRG1/2 via interaction with CONSTANS to modulate FT expression. PLoS Genet **10:** e1004617

Castelán-Muñoz N, Herrera J, Cajero-Sánchez W, Arrizubieta M, Trejo C, García-Ponce B, Sánchez MP, Álvarez-Buylla ER, Garay-Arroyo A (2019) MADS-box genes are key components of genetic regulatory networks involved in abiotic stress and plastic developmental responses in plants. Front Plant Sci **10:** 853

Chang G, Wang C, Kong X, Chen Q, Yang Y, Hu X (2018) AFP2 as the novel regulator breaks high-temperature-induced seeds secondary dormancy through ABI5 and SOM in *Arabidopsis thaliana*. Biochem Biophys Res Commun **501:** 232–238

Chen J, Mohan R, Zhang Y, Li M, Chen H, Palmer IA, Chang M, Qi G, Spoel SH, Mengiste T, et al (2019a) NPR1 promotes its own and target gene expression in plant defense by recruiting CDK8. Plant Physiol **181:** 289–304

Chen Z, Huang Y, Yang W, Chang G, Li P, Wei J, Yuan X, Huang J, Hu X (2019b) The hydrogen sulfide signal enhances seed germination tolerance to high temperatures by retaining nuclear COP1 for HY5 degradation. Plant Sci **285:** 34–43

Clough SJ, Bent AF (1998) Floral dip: A simplified method for *Agrobacterium*-mediated transformation of *Arabidopsis thaliana*. Plant J **16:** 735–743

Dai M, Xue Q, Mccray T, Margavage K, Chen F, Lee JH, Nezames CD, Guo L, Terzaghi W, Wan J, et al (2013) The PP6 phosphatase regulates ABI5 phosphorylation and abscisic acid signaling in Arabidopsis. Plant Cell **25:** 517–534

de la Paz Sanchez M, Gutierrez C (2009) Arabidopsis ORC1 is a PHD-containing H3K4me3 effector that regulates transcription. Proc Natl Acad Sci USA **106:** 2065–2070

Donohue K, Dorn L, Griffith C, Kim E, Aguilera A, Polisetty CR, Schmitt J (2005) Environmental and genetic influences on the germination of *Arabidopsis thaliana* in the field. Evolution **59:** 740–757

Finch-Savage WE, Leubner-Metzger G (2006) Seed dormancy and the control of germination. New Phytol **171:** 501–523

Finkelstein R, Reeves W, Ariizumi T, Steber C (2008) Molecular aspects of seed dormancy. Annu Rev Plant Biol **59:** 387–415

Garcia ME, Lynch T, Peeters J, Snowden C, Finkelstein R (2008) A small plant-specific protein family of ABI five binding proteins (AFPs) regulates stress response in germinating *Arabidopsis* seeds and seedlings. Plant Mol Biol **67:** 643–658

González-Morales SI, Chávez-Montes RA, Hayano-Kanashiro C, Alejo-Jacuinde G, Rico-Cambron TY, de Folter S, Herrera-Estrella L (2016) Regulatory network analysis reveals novel regulators of seed desiccation tolerance in *Arabidopsis thaliana*. Proc Natl Acad Sci USA **113:** E5232–E5241

Graeber K, Nakabayashi K, Miatton E, Leubner-Metzger G, Soppe WJ (2012) Molecular mechanisms of seed dormancy. Plant Cell Environ **35:** 1769–1786

Gu D, Chen CY, Zhao M, Zhao L, Duan X, Duan J, Wu K, Liu X (2017) Identification of HDA15-PIF1 as a key repression module directing the transcriptional network of seed germination in the dark. Nucleic Acids Res **45:** 7137–7150

Holdsworth MJ, Bentsink L, Soppe WJ (2008) Molecular networks regulating Arabidopsis seed maturation, after-ripening, dormancy and germination. New Phytol **179:** 33–54

Hu X, Kong X, Wang C, Ma L, Zhao J, Wei J, Zhang X, Loake GJ, Zhang T, Huang J, et al (2014) Proteasome-mediated degradation of FRIGIDA modulates flowering time in Arabidopsis during vernalization. Plant Cell **26:** 4763–4781

Hu Y, Han X, Yang M, Zhang M, Pan J, Yu D (2019) The transcription factor INDUCER OF CBF EXPRESSION1 interacts with ABSCISIC ACID INSENSITIVE5 and DELLA proteins to fine-tune abscisic acid signaling during seed germination in Arabidopsis. Plant Cell **31:** 1520–1538

Huo H, Dahal P, Kunusoth K, McCallum CM, Bradford KJ (2013) Expression of 9-cis-EPOXYCAROTENOID DIOXYGENASE4 is essential for thermoinhibition of lettuce seed germination but not for seed development or stress tolerance. Plant Cell **25:** 884–900

Jang JC (2016) Arginine-rich motif-tandem CCCH zinc finger proteins in plant stress responses and post-transcriptional regulation of gene expression. Plant Sci **252:** 118–124

Jing Y, Guo Q, Lin R (2019) The chromatin-remodeling factor PICKLE antagonizes polycomb repression of FT to promote fowering. Plant Physiol **181:** 656–668

Karssen CM, Brinkhorst-van der Swan DL, Breekland AE, Koornneef M (1983) Induction of dormancy during seed development by endogenous abscisic acid: Studies on abscisic acid deficient genotypes of *Arabidopsis thaliana* (L.) Heynh. Planta **157:** 158–165

Kim DH, Yamaguchi S, Lim S, Oh E, Park J, Hanada A, Kamiya Y, Choi G (2008) SOMNUS, a CCCH-type zinc finger protein in Arabidopsis, negatively regulates light-dependent seed germination downstream of PIL5. Plant Cell **20:** 1260–1277

Koornneef M, Jorna ML, Brinkhorst-van der Swan DL, Karssen CM (1982) The isolation of abscisic acid (ABA) deficient mutants by selection of induced revertants in non-germinating gibberellin sensitive lines of *Arabidopsis thaliana* (L.) Heynh. Theor Appl Genet **61:** 385–393

Koornneef M, van der Veen JH (1980) Induction and analysis of gibberellin sensitive mutants in *Arabidopsis thaliana* (L.) Heynh. Theor Appl Genet **58:** 257–263

Kucera B, Cohn MA, Leubner-Metzger G (2005) Plant hormone interactions during seed dormancy release and germination. Seed Sci Res **15:** 281–307

Laity JH, Lee BM, Wright PE (2001) Zinc finger proteins: New insights into structural and functional diversity. Curr Opin Struct Biol **11:** 39–46

Lee S, Cheng H, King KE, Wang W, He Y, Hussain A, Lo J, Harberd NP, Peng J (2002) Gibberellin regulates Arabidopsis seed germination via RGL2, a GAI/RGA-like gene whose expression is up-regulated following imbibition. Genes Dev **16:** 646–658

Lefebvre V, North H, Frey A, Sotta B, Seo M, Okamoto M, Nambara E, Marion-Poll A (2006) Functional analysis of Arabidopsis NCED6 and NCED9 genes indicates that ABA synthesized in the endosperm is involved in the induction of seed dormancy. Plant J **45:** 309–319

Li Z, Fu X, Wang Y, Liu R, He Y (2018) Polycomb-mediated gene silencing by the BAH-EMF1 complex in plants. Nat Genet **50:** 1254–1261

Lim S, Park J, Lee N, Jeong J, Toh S, Watanabe A, Kim J, Kang H, Kim DH, Kawakami N, et al (2013) ABA-insensitive3, ABA-insensitive5, and DELLAs interact to activate the expression of SOMNUS and other high-temperature-inducible genes in imbibed seeds in Arabidopsis. Plant Cell **25:** 4863–4878

López-González L, Mouriz A, Narro-Diego L, Bustos R, Martínez-Zapater JM, Jarillo JA, Piñeiro M (2014) Chromatin-dependent repression of the Arabidopsis floral integrator genes involves plant specific PHD-containing proteins. Plant Cell **26:** 3922–3938

Lopez-Molina L, Mongrand S, Kinoshita N, Chua NH (2003) AFP is a novel negative regulator of ABA signaling that promotes ABI5 protein degradation. Genes Dev **17:** 410–418

Majee M, Kumar S, Kathare PK, Wu S, Gingerich D, Nayak NR, Salaita L, Dinkins R, Martin K, Goodin M, et al (2018) KELCH F-BOX protein positively influences Arabidopsis seed germination by targeting PHYTOCHROME-INTERACTING FACTOR1. Proc Natl Acad Sci USA **115:** E4120–E4129

Matakiadis T, Alboresi A, Jikumaru Y, Tatematsu K, Pichon O, Renou JP, Kamiya Y, Nambara E, Truong HN (2009) The Arabidopsis abscisic acid catabolic gene CYP707A2 plays a key role in nitrate control of seed dormancy. Plant Physiol **149:** 949–960

Mathews S (2006) Phytochrome-mediated development in land plants: Red light sensing evolves to meet the challenges of changing light environments. Mol Ecol **15:** 3483–3503

Mazer SJ (1999) Seeds: Ecology, biogeography, and evolution of dormancy and germination. Science **283:** 334

Narro-Diego L, López-González L, Jarillo JA, Piñeiro M (2017) The PHD-containing protein EARLY BOLTING IN SHORT DAYS regulates seed dormancy in Arabidopsis. Plant Cell Environ **40:** 2393–2405

Ogawa M, Hanada A, Yamauchi Y, Kuwahara A, Kamiya Y, Yamaguchi S (2003) Gibberellin biosynthesis and response during Arabidopsis seed germination. Plant Cell **15:** 1591–1604

Park J, Lee N, Kim W, Lim S, Choi G (2011) ABI3 and PIL5 collaboratively activate the expression of SOMNUS by directly binding to its promoter in imbibed Arabidopsis seeds. Plant Cell **23:** 1404–1415

Penfield S, Li Y, Gilday AD, Graham S, Graham IA (2006) Arabidopsis ABA INSENSITIVE4 regulates lipid mobilization in the embryo and reveals repression of seed germination by the endosperm. Plant Cell **18:** 1887–1899

Peng M, Li Z, Zhou N, Ma M, Jiang Y, Dong A, Shen WH, Li L (2018) Linking PHYTOCHROME-INTERACTING FACTOR to histone modification in plant shade avoidance. Plant Physiol **176:** 1341–1351

Piñeiro M, Gómez-Mena C, Schaffer R, Martínez-Zapater JM, Coupland G (2003) EARLY BOLTING IN SHORT DAYS is related to chromatin remodeling factors and regulates flowering in Arabidopsis by repressing FT. Plant Cell **15:** 1552–1562

Piskurewicz U, Jikumaru Y, Kinoshita N, Nambara E, Kamiya Y, Lopez-Molina L (2008) The gibberellic acid signaling repressor RGL2 inhibits Arabidopsis seed germination by stimulating abscisic acid synthesis and ABI5 activity. Plant Cell **20:** 2729–2745

Quail PH (2002) Photosensory perception and signalling in plant cells: New paradigms? Curr Opin Cell Biol **14:** 180–188

Rajjou L, Duval M, Gallardo K, Catusse J, Bally J, Job C, Job D (2012) Seed germination and vigor. Annu Rev Plant Biol **63:** 507–533

Schwember AR, Bradford KJ (2010) A genetic locus and gene expression patterns associated with the priming effect on lettuce seed germination at elevated temperatures. Plant Mol Biol **73:** 105–118

Seo M, Aoki H, Koiwai H, Kamiya Y, Nambara E, Koshiba T (2004) Comparative studies on the Arabidopsis aldehyde oxidase (AAO) gene family revealed a major role of AAO3 in ABA biosynthesis in seeds. Plant Cell Physiol **45:** 1694–1703

Shu K, Liu XD, Xie Q, He ZH (2016) Two faces of one seed: Hormonal regulation of dormancy and germination. Mol Plant **9:** 34–45

Sun TP, Kamiya Y (1994) The Arabidopsis GA1 locus encodes the cyclase ent-kaurene synthetase A of gibberellin biosynthesis. Plant Cell **6:** 1509–1518

Talon M, Koornneef M, Zeevaart JA (1990) Endogenous gibberellins in *Arabidopsis thaliana* and possible steps blocked in the biosynthetic pathways of the semidwarf ga4 and ga5 mutants. Proc Natl Acad Sci USA **87:** 7983–7987

Toh S, Imamura A, Watanabe A, Nakabayashi K, Okamoto M, Jikumaru Y, Hanada A, Aso Y, Ishiyama K, Tamura N, et al (2008) High temperature-induced abscisic acid biosynthesis and its role in the inhibition of gibberellin action in Arabidopsis seeds. Plant Physiol **146:** 1368–1385

Wang Y, Gu X, Yuan W, Schmitz RJ, He Y (2014) Photoperiodic control of the floral transition through a distinct polycomb repressive complex. Dev Cell **28:** 727–736

Wysocka J, Swigut T, Xiao H, Milne TA, Kwon SY, Landry J, Kauer M, Tackett AJ, Chait BT, Badenhorst P, et al (2006) A PHD finger of NURF couples histone H3 lysine 4 trimethylation with chromatin remodelling. Nature **442:** 86–90

Xu D, Li J, Gangappa SN, Hettiarachchi C, Lin F, Andersson MX, Jiang Y, Deng XW, Holm M (2014a) Convergence of light and ABA signaling on the ABI5 promoter. PLoS Genet **10:** e1004197

Xu Y, Gan ES, Zhou J, Wee WY, Zhang X, Ito T (2014b) Arabidopsis MRG domain proteins bridge two histone modifications to elevate expression of flowering genes. Nucleic Acids Res **42:** 10960–10974

Xu YL, Li L, Wu K, Peeters AJ, Gage DA, Zeevaart JA (1995) The GA5 locus of *Arabidopsis thaliana* encodes a multifunctional gibberellin 20-oxidase: Molecular cloning and functional expression. Proc Natl Acad Sci USA **92:** 6640–6644

Yamaguchi S (2008) Gibberellin metabolism and its regulation. Annu Rev Plant Biol **59:** 225–251

Yang W, Chen Z, Huang Y, Chang G, Li P, Wei J, Yuan X, Huang J, Hu X (2019) Powerdress as the novel regulator enhances Arabidopsis seeds germination tolerance to high temperature stress by histone modification of SOM locus. Plant Sci **284:** 91–98

Yang Z, Qian S, Scheid RN, Lu L, Chen X, Liu R, Du X, Lv X, Boersma MD, Scalf M, et al (2018) EBS is a bivalent histone reader that regulates floral phase transition in Arabidopsis. Nat Genet **50:** 1247–1253